Pohl, E., Gloaguen, R., Andermann, C., Knoche, M. (2017): Glacier melt buffers river runoff in the Pamir Mountains. - *Water Resources Research*, *53*, 3, pp. 2467—2489.

DOI: http://doi.org/10.1002/2016WR019431

AGU PUBLICATIONS

Water Resources Research

RESEARCH ARTICLE

10.1002/2016WR019431

Glacier melt buffers river runoff in the Pamir Mountains

Eric Pohl[1], Richard Gloaguen[1], Christoff Andermann[2], and Malte Knoche[3]

[1]Helmholtz-Zentrum Dresden-Rossendorf, Helmholtz Institute Freiberg for Resource Technology, Division Exploration Technology, Freiberg, Germany, [2]Helmholtz Centre Potsdam, German Research Centre for Geosciences, Potsdam, Germany, [3]Helmholtz Centre for Environmental Research, Halle, Germany

Key Points:
- Upscaling of regional hydrological model to the greater Pamir area using multisource validation data
- Glaciers buffer extreme meteorological events and provide sustainable river runoff
- Regional climatic differences substantially affect the hydrological cycle and its evolution

Supporting Information:
- Supporting Information S1

Correspondence to:
E. Pohl,
e.pohl@hzdr.de

Citation:
Pohl, E., R. Gloaguen, C. Andermann, and M. Knoche (2017), Glacier melt buffers river runoff in the Pamir Mountains, *Water Resour. Res.*, *53*, 2467–2489, doi:10.1002/2016WR019431.

Received 8 JUL 2016
Accepted 23 FEB 2017
Accepted article online 2 MAR 2017
Published online 29 MAR 2017

Abstract Newly developed approaches based on satellite altimetry and gravity measurements provide promising results on glacier dynamics in the Pamir-Himalaya but cannot resolve short-term natural variability at regional and finer scale. We contribute to the ongoing debate by upscaling a hydrological model that we calibrated for the central Pamir. The model resolves the spatiotemporal variability in runoff over the entire catchment domain with high efficiency. We provide relevant information about individual components of the hydrological cycle and quantify short-term hydrological variability. For validation, we compare the modeled total water storages (TWS) with GRACE (Gravity Recovery and Climate Experiment) data with a very good agreement where GRACE uncertainties are low. The approach exemplifies the potential of GRACE for validating even regional scale hydrological applications in remote and hard to access mountain regions. We use modeled time series of individual hydrological components to characterize the effect of climate variability on the hydrological cycle. We demonstrate that glaciers play a twofold role by providing roughly 35% of the annual runoff of the Panj River basin and by effectively buffering runoff both during very wet and very dry years. The modeled glacier mass balance (GMB) of -0.52 m w.e. yr^{-1} (2002–2013) for the entire catchment suggests significant reduction of most Pamiri glaciers by the end of this century. The loss of glaciers and their buffer functionality in wet and dry years could not only result in reduced water availability and increase the regional instability, but also increase flood and drought hazards.

Plain Language Summary Glaciers store large amounts of water in the form of ice. They grow and shrink dominantly in response to climatic conditions. In Central Asia, where rivers originate in the high mountains, glaciers are an important source for sustainable water availability. Thus, understanding the link between climate, hydrology, and glacier evolution is fundamental. Some instruments mounted on satellites are capable of monitoring glaciers. However, the potential of these sensors is limited by technical constraints that will affect the availability and precision of the products. In order to overcome these shortcomings and investigate glacier dynamics, we use a numerical model that represents the relevant processes of the hydrological cycle with a very fine spatial and temporal resolution. We validate model results with snow cover observations and measurements of the total amount of water stored in the region. We demonstrate that this approach is valid and could facilitate studies in other cold climate regions. Our results show that glaciers buffer extreme weather conditions to provide sustainable river flow. This functionality is put in jeopardy due to the currently observed glacier retreat, in the Pamir Mountains.

1. Introduction

The Pamir Mountains constitute the source of water resources for irrigation, hydropower, and drinking water for a large part of Central Asia. The main draining river is the Amu-Darya, which water resources are subject of an ongoing trans-boundary water allocation conflict [*Bernauer and Siegfried*, 2012; *Varis*, 2014]. The shrinkage of the Aral Sea is just the most prominent aspect of the conflictual relations between the riparian countries. Climate-change induced impacts on water availability, may increase political instability and threaten livelihoods and thus become particularly prominent issues in mountainous regions [*Gleick and Heberger*, 2014; *Bhatta et al*., 2015]. The fate of the high mountain water resources in the western end of the Himalayas is especially unclear in a warming climate [*Unger-Shayesteh et al*., 2013; *Immerzeel et al*., 2010]. One of the main reasons for that is data scarcity and the poorly constrained hydrological cycle. The snowmelt-dominated and glacier-melt-dominated runoff regime is expected to be sensitive to changes

in temperatures, which will affect glacier mass balance, the distribution of rain/snow, and the generation of runoff from snowmelt in the westernmost parts of the Himalayas [*Kure et al*., 2013a; *Tahir et al*., 2011; *Lutz et al*., 2014; *Pohl et al*., 2015a]. Trends toward decreasing snow cover duration and increasing temperatures are apparent in Central Asia [*Dietz et al*., 2014; *Aizen et al*., 1997; *Makhmadaliev et al*., 2008] and it is expected that these changes will cause a shift in seasonality as well as an eventual reduction of glacier melt contribution to runoff [*Hagg et al*., 2013; *Kure et al*., 2013a]. The consequences of glacier shrinkage have not yet been investigated at the temporal and spatial scales that would allow setting up water management strategies on local scales for the entire Pamir.

Glaciological studies generally reported glacier retreat or glacier mass loss in the greater Pamir region [*Kääb et al*., 2015; *Sorg et al*., 2012; *Lutz et al*., 2013; *Bolch et al*., 2012] although parts in the Pamir and the Karakoram display slight mass gain [*Gardelle et al*., 2013]. The spatial heterogeneity in glacier evolution in the Pamir is partly inherent from precipitation gradients and seasonality [*Fuchs et al*., 2013; *Pohl et al*., 2015b] although this does not account for short-term local meteorological conditions that can play a crucial role [*Mölg et al*., 2012; *Liu et al*., 2014; *Khromova et al*., 2006]. This is important to note because the assessment of glacier evolution is often based on very few observations due to the limited availability of adequate remote sensing products. An accurate assessment of climate variability or persistent trends and their effects on glacier evolution and hydrology is thus difficult in regions with no or limited in situ measurements. The greater Pamir region experiences strong interannual climate variability [*Pohl et al*., 2015b; *Kapnick et al*., 2014]. In a previous study, we have shown that the spatiotemporal interplay of precipitation and temperature can generate conditions that lead to regional floods in 1 year and severe droughts in the following year [*Pohl et al*., 2015b]. This variability consequently raises the question whether observed trends, based on a few observations in time, reflect a representative evolution of glaciers and the hydrological system. The discrimination between long-term trends and variability, however, is required for sound future projections.

To evaluate variations of the hydrological cycle that are related to a change in climatic forcing, we have developed a hydrological model for a representative catchment in the central Pamir, the Gunt River ($\sim$14,000 km^2). We tested several state-of-the art remote sensing, regional climate model (RCM), and interpolated data sets to validate their usefulness in a hydrological application where the lack of situ data demands for alternative approaches [*Pohl et al*., 2015a]. In the present study, we upscale and validate the small-scale model to the entire Panj River catchment ($\sim$77,000 km^2) that comprises most of the high Pamir Mountains. Special focus is set on the discrimination between regional scale differences in the Panj catchment and the expected effects of climate change and climate variability on glacier mass balances and water availability. The large-scale modeling facilitates comparison of modeled total water storages (TWS) with data derived from the Gravity Recovery And Climate Experiment (GRACE) [*Landerer and Swenson*, 2012; *Swenson and Wahr*, 2006]. In return, models providing information on TWS and glacier dynamics can help improve the estimates of land-surface-atmosphere interactions that are required to process GRACE data to estimate TWS changes accurately [*Long et al*., 2015; *Güntner et al*., 2007]. GRACE TWS can provide an independent data source for the validation and hydrological investigations but its large footprint limits this application to sufficiently large regions [*Farinotti et al*., 2015; *Sproles et al*., 2015; *Tangdamrongsub et al*., 2015]. Land surface models (LSM) are currently used to provide estimates for land-surface-atmosphere interactions but usually do not discriminate storage components such as groundwater and glaciers. The aims of this study are hence (1) to evaluate the model-upscaling to the entire Panj drainage basin, (2) to test whether regional differences in glacier mass balance [*Kääb et al*., 2015] can be captured with our approach and to highlight the associated hydroclimatological characteristics at regional scale, and (3) to validate the usefulness of GRACE for glaciohydrological modeling under data scarcity. Ultimately, we want to (4) assess the quantitative impact of climate variability compared to long-term trends in climate change and the implications for future water management.

2. Study Area

The Panj River (which is called Amu Darya downstream in the Tajik basin) originates in the Pamir Mountains and has a catchment size of approximately 77,000 km^2. The elevation ranges between 800 m a.s.l. at Khirmandkho, where a river gauging station is located at the Panj River, and more than 7000 m a.s.l. at the

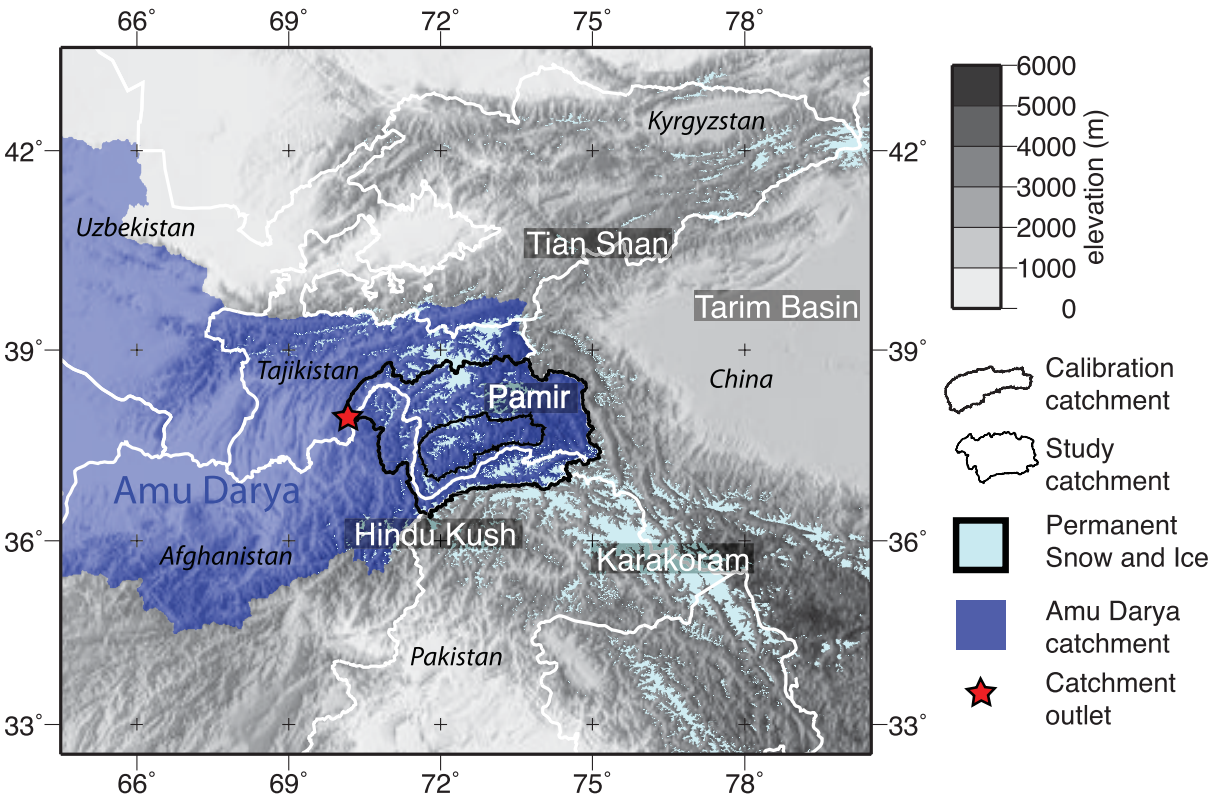

Figure 1. Amu Darya river catchment and the subcatchment with gauging station at site Khirmandkho. Glacier cover is approximated by means of MODIS MCD12Q1 land cover data.

catchment boundaries in the north and south and at the mountain ridges in the central part. The mean elevation is 4000 m a.s.l. A prominent precipitation gradient in west-east direction is accompanied by higher glaciation in the west than in the eastern part. Precipitation shows a distinct seasonality with high intensity snowfall during winter and spring and little summer precipitation. The deflection of westerly trade winds at the western orogen margin to the north and to the south cause intense precipitation at the margins and arid conditions in the eastern Pamir (Figure 2) [*Fuchs et al.*, 2013; *Pohl et al.*, 2015b]. About 85% of precipitation is supplied as snow during winter [*Pohl et al.*, 2015a]. Moisture supply is driven by the synoptic-scale circulation of the Westerlies in winter from west to east, and less constrained northward and southward intrusions of the Indian summer monsoon (ISM), and northern intrusions in summer [*An et al.*, 2012; *Aizen et al.*, 2009; *Schiemann et al.*, 2007].

While the mechanisms and sources leading to summer precipitations are debated, they account for a small fraction of the total annual precipitation amount in the central and western parts of the Pamir. The Gunt catchment, which was used for calibration of the model [*Pohl et al.*, 2015a] (Figure 1), is characterized by the same gradient in precipitation and glaciation as the Pamir in general [*Fuchs et al.*, 2015; *Pohl et al.*, 2015a]. Decreasing glaciation and less precipitation towards the east directly imply locally variable runoff magnitudes.

Runoff shows a distinct seasonality with steady low flow in winter, a rapid runoff increase in spring, high peak flow with strong variability during summer, and a sharp decline in early autumn. About 40% of the annual runoff in the central Pamir results from groundwater discharge, which is essentially the only contributor to stream flow in winter [*Pohl et al.*, 2015a]. About 30% of the annual runoff is glacier melt (snow and ice), which limits the overall contribution to total stream flow of non/little-glaciated catchments in late summer. In order to validate the upscaling, we obtained discharge data for five additional catchments that cover different parts of the Pamir and reflect different glaciation and precipitation regimes (Figure 3). The northernmost river catchments (Vanj and Bartang) show extensive glaciation. The large drainage basin

(Shidz) excludes the areas with high precipitation amounts in the northwestern Pamir. The eastern Pamir drains into Sarez Lake, which is located immediately before the gauging station Nisur at the Bartang River. Lake Sarez has only a subsurface outflow from its natural dam, with an almost constant discharges of ≈40 $m^3 s^{-1}$ and little seasonal variability. The available time series of in situ discharge of the Bartang station exclude this discharge of Lake Sarez's outlet.

Permanent snow and ice cover represent ≈13%, barren or sparsely vegetated ≈58% and grassland ≈28% of the land cover within the Panj River basin (according to MODIS MCD12Q1 land cover data set, *Strahler et al*. [1999]). Strongly incised valleys with steep slopes and high winter precipitation at the western margin constitute a hazard potential for snow and ice avalanches, rockslides, and debris flows [*Gruber and Mergili*, 2013].

3. Methods

We use the J2000g hydrological model [*Kralisch et al*., 2007; *Krause and Hanisch*, 2009], as in our previous local study [*Pohl et al*., 2015a], in which we evaluated currently available state-of-the-art gridded meteorological data sets. We derived meaningful calibration parameters with respect to the data set's original spatial resolutions and the calibration catchment's variability in precipitation and morphology. This variability is also observed at bigger scale for the greater Pamir region, i.e., a strong precipitation gradient from the deeply incised western parts to the arid, and gentle hillslope, high altitude plateau in the east. We use the same model parameterization; however, some changes were made in the data sets used (cf. following section). We do not perform any spatial resampling on the data sets to limit the computational expense and explore the possibility to directly use such data for the large-scale application.

J2000g is a simple, semidistributed hydrological model. It uses a small number of calibration parameters and thus facilitates application in environments where little information about soil and hydrogeological properties are available. J2000g does not use water routing in a topological context, but calculates the hydrological water balance for each hydrological response unit (HRU) individually. Calculated runoff components are summed up in the end to yield the total runoff (Q_{tot}). The calibration parameters and their values obtained from the previous modeling are given in Table 1.

The water balance is calculated using the following briefly described routine. Net radiation is calculated based on *Allen et al*. [1998], followed by the calculation of potential evaporation (potET) after Penman-Monteith. Based on a threshold temperature *Tbase*, precipitation is discriminated as rain or snow. Snow and ice melt are calculated based on a day-degree method. A total of three time-degree-factors (TMF) are used: one for snow of nonglaciated HRUs, and two for snow and ice of glaciated HRUs, respectively. Glacier mass balance is calculated as the difference between precipitation input and runoff from snow and ice of glacier HRUs. Glacier runoff is the sum of snow and glacier melt, and rainfall runoff from glaciated HRUs and is treated as direct runoff (Q_{dir}), which cannot infiltrate into soils and the groundwater component. For nonglaciated HRUs, meltwater and liquid precipitation are transferred to the soil water module. The module

Table 1. Model Parameterization Obtained for the Gunt Catchment and Applied to the Greater Pamir Region and Their Description

Parameter	Calibrated Value	Description
Tbase	5.01°C	Threshold temperature for freezing/melting of nonglaciated HRUs
TMF_s	4.31 mm $°C^{-1}$ d^{-1}	Degree-day factor for snowmelt of nonglaciated HRUs
$Tbase_g$	0.96°C	Threshold temperature for freezing/melting of glaciated HRUs
TMF_{gs}	4.07 mm $°C^{-1}$ d^{-1}	Degree-day factor for snowmelt of glaciated HRUs
TMF_{gi}	0.89 mm $°C^{-1}$ d^{-1}	Degree-day factor for ice melt of glaciated HRUs
ETR	0.45	Evapotranspiration reduction factor accounting for increasing resistance against evapotranspiration with decreasing soil moisture content
maxPerc	12.08	Scaling factor for maximum percolation rates
LVD	1.26×10^{-3}	Lateral-vertical distribution; lower values for more vertical and less lateral flow
FCA	3.56×10^{-2}	Field-capacity adaption; lower values for less field capacity
gwStorAlpha	0.41	Distribution coefficient of percolation to either groundwater storage components; lower values for higher contribution to deep groundwater and less contribution to fast recession component
GWK1	19.16 days	Recession parameter for the first linear storage (fast subsurface flow)
GWK2	216.49 days	Recession parameter for the second linear storage (deep groundwater)

prevents percolation water unless saturation is reached. This definition did not account for poorly evolved soils in the Pamir, where coarse sediment deposits provide little water withholding capacity [*Pohl et al*., 2015a]. An additional linear storage component (GW1) was therefore introduced, which resembles the expected retardation effects and complements the deeper groundwater flow (GW2). The main purpose of the soil module in its current form is to provide the interface for evapotranspiration. An evapotranspiration reduction factor ETR accounts for uncertainties in the physical representation of the soils and vegetation. The introduction of two linear storage components resulted in low values for the soil calibration parameters FCA (water storage capacity) and LVD (Lateral-Vertical-Distribution). These values cause the bulk of water to be transferred to the underlying storage components GW1, and the deeper groundwater storage component GW2. Both of these underlying components release water with delay, which is simulated by linear recession coefficients GWK1 and GWK2, respectively. The distribution of soil excess water to either GW1 or GW2 is determined by the distribution coefficient gwStorAlpha. In the end, Q_{dir} and the runoff of GW1 and GW2 (Q_{bas1}, and Q_{bas2}) of each HRU are summed up to give the total simulated streamflow Q_{tot}.

4. Data

Data sets used in this study are described in more detail in *Pohl et al*. [2015a]. For precipitation, we use the High Asia Reanalysis (HAR) data set [*Maussion et al*., 2014] with 10 km spatial and daily temporal resolution for precipitation. The data result from a dynamical downscaling of global analysis data (Final Analysis data from the Global Forecasting System [*National Centers for Environmental Prediction NOAA, U.S. Department of Commerce*, 2000]; data set ds083.2) using the Weather Research and Forecasting (WRF-ARW) model [*Skamarock and Klemp*, 2008]. This data set shows high consistency with other meteorological parameters, such as snow cover and is able to capture climatic interactions in the greater Pamir region that can lead to floods and droughts [*Pohl et al*., 2015b]. The data set is increasingly used for glacier studies in the greater Himalayan region [*Maussion et al*., 2011; *Mölg et al*., 2013; *Curio et al*., 2015]. We have shown the crucial need to bias-correct HAR precipitation intensities in the Pamir [*Pohl et al*., 2015a], as has *Biskop et al*. [2016] for the Tibetan Plateau. A similar procedure is needed for several data sets in the data sparse Central Asian mountains [e.g., *Duethmann et al*., 2013]. We use the same intensity downscaling (factor 0.37) we validated in our previous study. The spatial domain of the 10 km spatial resolution HAR data set does not completely cover the study area. Therefore, we merge the 30 km and 10 km versions HAR30 and HAR10 (Figure 2). These data sets are highly consistent with respect to intensities and spatiotemporal distribution.

For temperature, we use the MODIS MOD11C1 V5 land surface temperature (LST) data set [*Wan and Li*, 1997; *Wan et al*., 2004; *Wan*, 2008], which shows strong correlation with in situ 2 m air temperature data [*Pohl et al*., 2015a]. We calibrated MODIS MOD11C1 V5 night LST with in situ measurements and used it as a proxy for air temperature. We further use ECMWF (European Centre for Medium-Range Weather Forecast) ERA-Interim [*Dee et al*., 2011] sunshine duration data in 0.75 × 0.75° spatial resolution. The data are needed by the model internal calculation of global radiation and serves as a proxy for cloudiness to reduce the internally calculated extraterrestrial radiation. For relative humidity and wind speed, we use output of the HAR data set, which provides a superior spatial resolution to the previous data sources. For soil properties, we now use only information from the Harmonized World Soil Database (HWSD) [*FAO et al*., 2009].

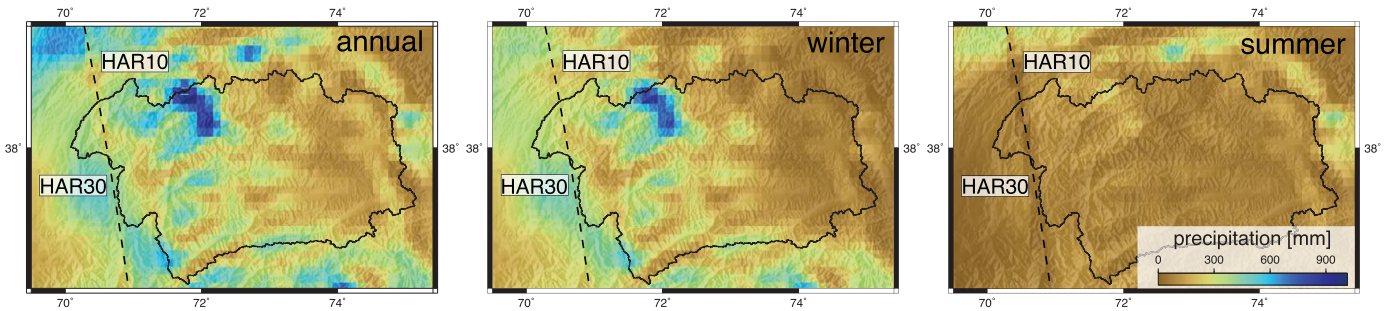

Figure 2. Mean annual, winter (NDJFMA), and summer (MJJASO) precipitation amounts of the merged HAR10 and HAR30 data sets (2001 to 2013). The dashed line indicates the spatial domains of HAR10 and HAR30, respectively. HAR30 data were resampled to the spatial resolution of HAR10 and merged with HAR10 data to cover the westernmost part of the catchment area.

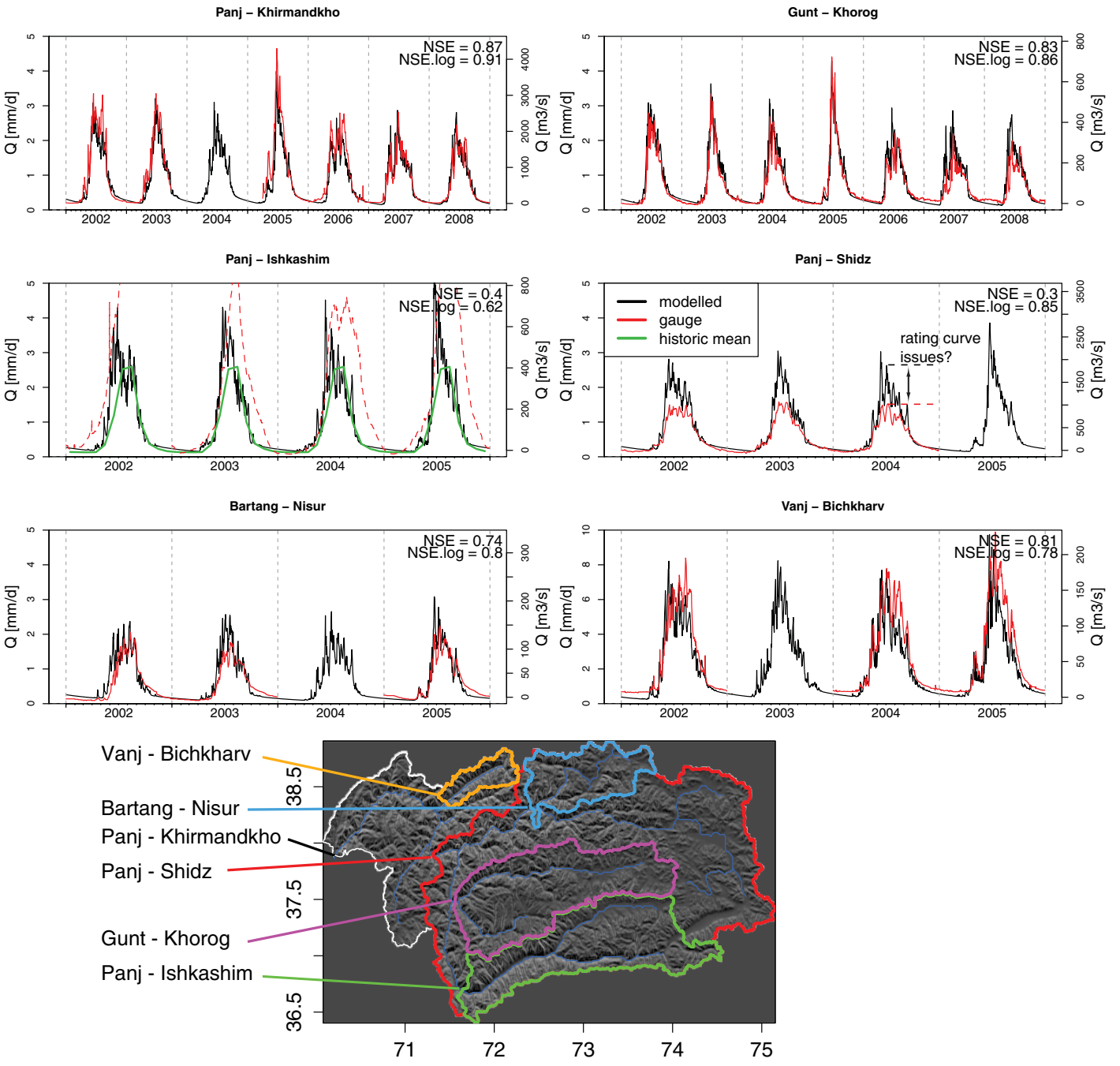

Figure 3. Model performance for different subcatchments. Unknown data quality for records in the 2000s (red dashed line) for Ishkashim shows inconsistency with historic monthly mean values. Shidz and Ishkashim are located at the Panj River at the boarder to Afghanistan. No recalibration for rating curves has been conducted here since 1991. The wide river bed might imply a possible source of error. Note the twofold higher amplitude in runoff for the Vanj River catchment Bichkharv. Bottom map shows location of individual subcatchments.

The changes have no noticeable impact on the obtained representation of the hydrograph and the obtained Nash-Sutcliffe efficiency (NSE) [*Nash and Sutcliffe*, 1970] for the Gunt catchment, for which the calibration parameters were obtained (Figure 3).

The large catchment scale facilitates incorporation of GRACE [*Landerer and Swenson*, 2012; *Swenson and Wahr*, 2006] data as an additional validation tool for the modeled water balance. It further helps to constrain the main hydrological compartments with minimum assumptions. An absence of constraints on these

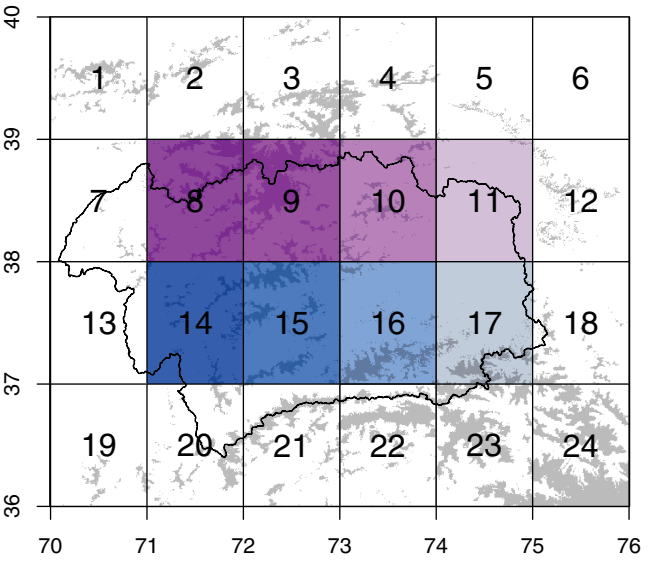

Figure 4. GRACE grid with assigned IDs superimposed on glacier extent (gray). Colored regions with significant overlap of modeled area (black outline) and GRACE pixels are used to highlight regional behaviour with respect to water components later on.

compartments (e.g., glaciers, precipitation) has complicated previous attempts to model the hydrologic cycle in the Pamir [e.g., *Hagg et al.*, 2013].

We utilize the GRACE product releases RL05.DSTvSCS1409 of the German Research Centre for Geoscience (GFZ), and the Center for Space Research (CSR), and product RL05.DSTvSCS1411 from the Jet Propulsion Laboratory (JPL) to see whether modeled TWS could be obtained through GRACE. GRACE RL05 data sets come in $1 \times 1°$ spatial (Figure 4) and monthly temporal resolution. The sampling and postprocessing of GRACE observations attenuate mass variations at local scale. Such variations are expected in the Pamir due to the strong seasonality and precipitation gradients. Therefore, we apply the scaling factors provided with the data sets in order to account for the attenuation [see *Landerer and Swenson*, 2012; *Long et al.*, 2015 for further information]. These scaling factors are calculated by applying a filtering method (applied to the GRACE data) to land surface models (LSM), with the goal to remove atmospheric and hydrological effects off the GRACE signal.

The scaling factor is usually given by the ratio of the filtered and unfiltered LSM signal. However, the LSMs operate at larger scale than our model and rely on climate forcing data, which might have high uncertainties in Pamir [e.g., *Palazzi et al.*, 2013]. Furthermore, the LSMs do not include groundwater or glacier storage changes. As a consequence, the resulting GRACE TWS anomalies (including the scaling factor) might not represent the strongly heterogenous hydrological conditions in the Pamir. Improvement of these issues is a focus of research [e.g., *Long et al.*, 2015]. GRACE data are increasingly being applied for glacial and hydrological studies [e.g., *Gardner et al.*, 2013; *Güntner et al.*, 2007; *Feng et al.*, 2013], even at regional scale [*Farinotti et al.*, 2015; *Sproles et al.*, 2015; *Tangdamrongsub et al.*, 2015]. We compare GRACE TWS with the total water storage (TWS) obtained through the modeling experience, i.e., the sum of the groundwater storages (GW1 + GW2), soil water storage, snow water storage, and changes in the glacier mass balance (without snow) and lakes. We recalculate GRACE TWS anomalies for the reference period 2002 to 2013 to match the period of our modeling. Daily TWS from the modeling was averaged to monthly values for comparison with GRACE data. We calculate anomalies as deviation from the long-term mean, as well as monthly anomalies, i.e., the deviation from the mean monthly values.

5. Validation and Sensitivity Analysis

For validation, we compare modeled Q_{tot} with observational data obtained from the State Administration for Hydrometeorology of Tajikistan (SAHT) (Figure 3). Extensive validation is impeded by the lack of recent data across the Tajik Pamir. After 1991, no recalculation of rating curves was performed along the Panj River. Furthermore, locally wide valleys (up to 400 m) and the inherent risk of taking in situ measurements during peak discharge events from hand cranked gondolas might have impeded accurate rating curves. We suggest that in situ data may locally have quality issues. These problems have been partially confirmed by our own experience during several visits to the measurement stations. This might explain the bad representation in terms of NSE for site Shidz during summer. NSE is significantly better based on logarithmic values and also in winter at low-flow conditions. We also encountered that discharge data are not consistent for different periods of acquisitions. For Ishkashim, most recent daily data would imply strong underestimation of modeled values, but historic monthly mean values have similar values to our model predictions (Figure 3). We thus

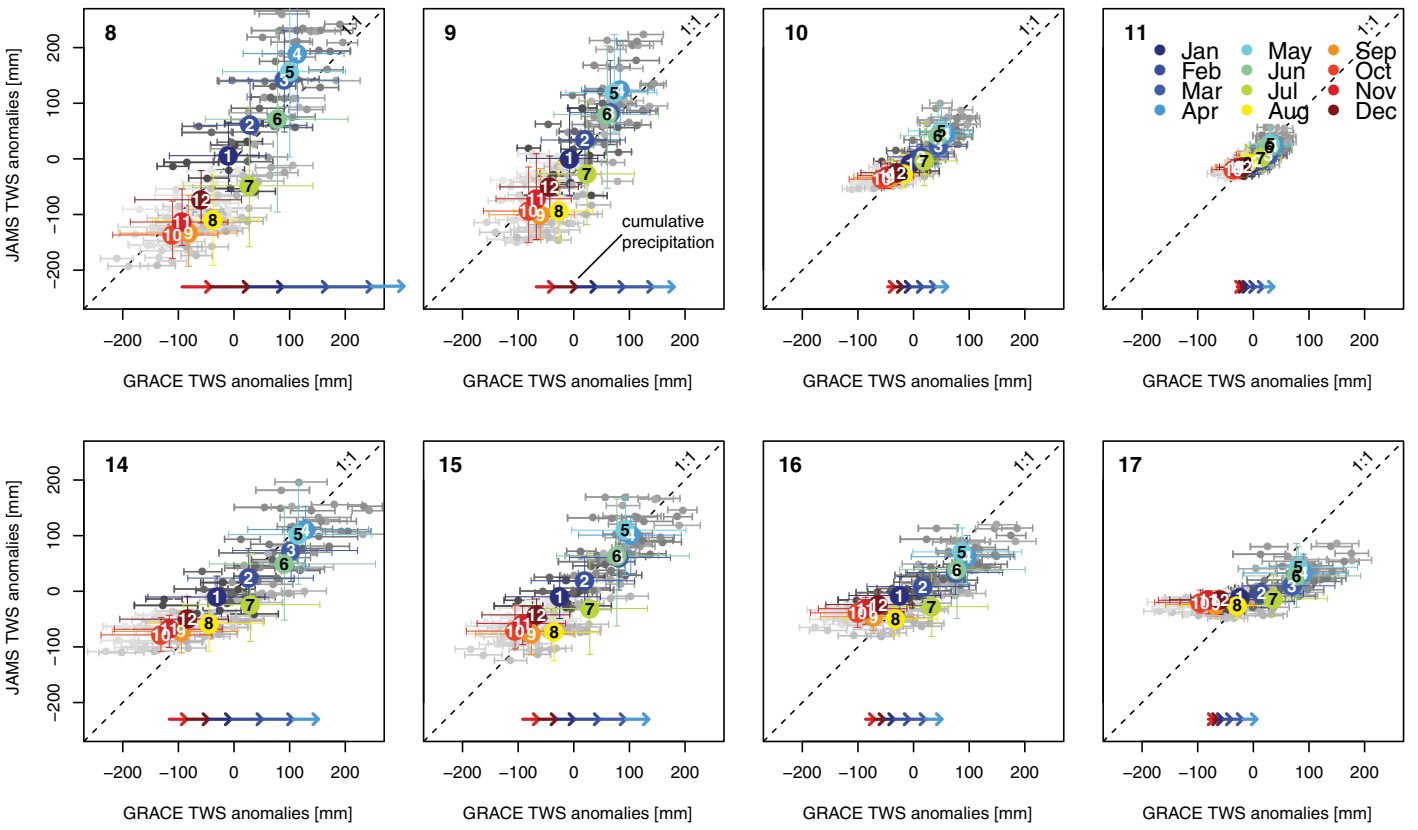

Figure 5. Comparison of modeled and GRACE monthly TWS anomalies (reference is the period 2002–2013). Individual plots refer to GRACE pixels in Figure 4. Gray-scale error bars represent the range of different GRACE solutions (GFZ, CSR, JPL) ±measurement error. Gray center dots are the mean of the GRACE solutions. Colored dots mark mean monthly values and colored error bars represent the full range of mean monthly values. Striking linear relationships for all sites between November and March. Colored arrows show the mean cumulative precipitation from November to April, starting at the mean monthly GRACE value for November. Length of arrows according to *x* axis scaling. Number (top-left) is the GRACE pixel-ID. Scales in all subfigures are constant to highlight regional differences in TWS.

question the validity of daily station data on the ground of the strong deviation from the long-term mean values. For the lowermost gauging station at Khirmandkho, the validation yields a NSE of 0.87 and 0.91 for logarithmic values, suggesting a very good representation of the hydrological cycle of the Pamir as a whole. The model is also able to capture the regional differences of twofold higher runoff at site Bichkharv, where HAR shows significantly higher precipitation (Figure 2), suggesting that HAR is able to represent spatial precipitation patterns in the Pamir accurately.

Comparison of monthly TWS anomalies from the model and GRACE is shown in Figure 5. Values plot mainly along the 1:1 line. Striking is a strong linear relationship from November to April for all sites, however with varying slopes. The mean cumulative precipitation for the same time period, indicated by the arrows in Figure 5, has the same magnitude as modeled TWS increase. Where modeled and GRACE TWS deviate the most from each other, cumulative precipitation is much lower than the indicated TWS changes from GRACE. This is particularly the case in the southeastern regions.

We tested the sensitivity of calibration parameters in the previous study [*Pohl et al.*, 2015a] with respect to varying precipitation amounts from three different data sets, and with respect to two different temperature data sets. We observe narrowly constrained value ranges for most of the calibration parameters (see supporting information S1, Figure S5). The use of either temperature data set had the lowest impact on the realizations of calibrated parameters. Precipitation intensities affected the realizations of $Tbase_g$ to start glacier melt earlier for data sets with low precipitation intensities, thus accounting for early depleted snow stocks. This further affected the realization of the two subsurface flow components. However, TMF_{gi} has been very precisely constrained to values around 1 mm $°C^{-1}$ d^{-1} for different precipitation data sets with annual cumulative precipitation amounts between 154 and 400 mm [*Pohl et al.*, 2015a].

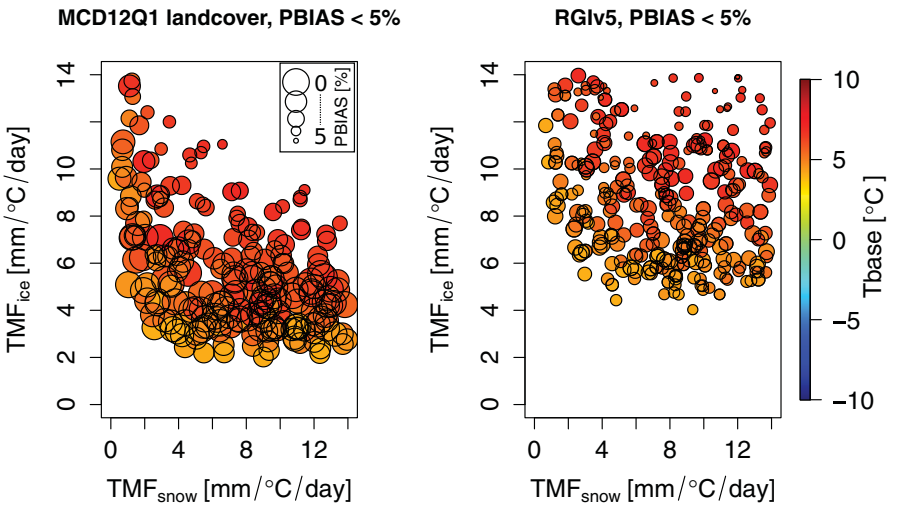

Figure 6. Possible TMF_{gi} and TMF_{gs} combinations for downscaled temperature data set (1×1 km) that reproduce glacier runoff of the original model (5×5 km). Displayed are combinations with a Tbase range between 4 and 7°C (according to calibrated Tbase values from *Pohl et al.* [2015a]), and where PBIAS < 5%. Effect of glacier cover data sets on the parameterization using MODIS MCD12Q1 (left), and RGIv5 (right) (see supporting information S2, Figure S7 for more details).

The direct use of 5×5 km spatial resolution temperature data homogenizes and simplifies the melting processes over large elevation bands. It also causes a temperature overestimation for highest, and an underestimation for lowest elevation bands (see supporting information S2, Figure S6). While this simplification is beneficial in terms of computational expense and yields high NSE, it has inevitable consequences for the calibration of the model parameters. To test our derived degree-day-factors for plausibility and identify respective value ranges if we had used a finer scaled temperature data set, we downscaled the 5×5 km temperature data to 1×1 km spatial resolution (see supporting information S2). Figure 6 shows the possible TMF_{gi}, and TMF_{gs} combinations that reproduce the total modeled glacier runoff (from glacier HRUs using the 5×5 km temperature data) with less than $\pm 5\%$ bias (PBIAS), using the Tbase range that was calibrated for the rest of the HRUs [*Pohl et al.*, 2015a] (supporting information S1). The most frequent values for TMF_{gi}, using the derived glacier area from the MCD12Q1 land cover data lie between 4 and 6 mm $°C^{-1}$ d^{-1}, and between 6 and 8 mm $°C^{-1}$ d^{-1} using the derived glacier area from the Randolph Glacier Inventory (RGI) version 5 [*Arendt et al.*, 2015], respectively (supporting information S2, Figure S7). These values are close to common literature values [*Hock*, 2003], and agree well with e.g., *Lutz et al.* [2014], highlighting a decisive role of the chosen temperature data resolution. The coarse temperature data resolution also affected the parameterization of Tbase in the calibration process. MODIS pixels average over areas that comprise higher altitudes than where the meteorological stations are located. Consequently, the calibrated data set shows higher values, which are compensated for by an increased Tbase (see supporting information S2 for more details).

Several studies have shown that implementing snow cover in the optimization function helps modeling the hydrological cycle in a more realistic way and to attribute issues in precipitation data [e.g., *Duethmann et al.*, 2014; *Finger et al.*, 2015]. We previously identified issues in the most commonly used precipitation data for the region through the multisource data approach and by the use of different correction factors for the precipitation data [*Pohl et al.*, 2015a]. Instead we perform here a comparison of monthly snow cover from the MODIS MOD10CM data set [*Hall et al.*, 2006] and modeled snow cover for 200 m altitude bands (see supporting information S3, Figure S8) for the individual regions. This comparison suggests a good representation of modeled and observed values. Highest uncertainties occur at lowest elevations for each of the regions. These uncertainties are expected with regard to the coarse resolution temperature and precipitation data that cannot resolve the local characteristics at the valley bottoms, nor account for wind drift snow redistribution in the arid eastern Pamir [cf. *Pohl et al.*, 2015a] (see section 7). All subsequent analyses are based on the model setup with the 5×5 km temperature data consistent with the approach of our preliminary work. Because the model parametrization was calibrated with the setup presented here, studies in other regions outside the study area will have to carefully evaluate if they are applicable there. The multisource

validation scheme supports our model estimates obtained with the presented choice of data sets, which favor ease of use and computational expense. However, there is also an inherent simplification of melting processes, which is why the results presented here provide first-order estimates subject to refinement in the future.

6. Results

Regional hydrometeorological conditions vary strongly across the Pamir. Figure 7 provides an overview of the spatiotemporal characteristics and trends. Highest variations in modeled runoff are apparent in a west-east direction. Mean annual values of 576 mm yr^{-1} in the northwest contrast 101 and 151 mm yr^{-1} in the east. The spatial variability in Q_{tot} reflects largely the variability in precipitation (Figure 2). However, a comparison of mean annual precipitation and Q_{tot} (Figure 7) reveals that Q_{tot} can be even higher than precipitation in the westernmost parts, while Q_{tot} is always lower than precipitation in the drier regions. Use of the MOD11C1 temperature data set reveals increasing trends in temperature across the study area. Strongest increases of 0.11°C yr^{-1} are apparent in the east and lowest ones of 0.07–0.08°C yr^{-1} in the north-eastern parts.

Because runoff, precipitation, and glacier mass balance show high-frequency signals that are difficult to visualize and interpret, we calculated the cumulative sums of these time series. From these cumulative signals, we calculated the detrended seasonal signals by performing a simple linear regression over time. We then calculated daily anomalies of the detrended time series, i.e., the deviation from the mean daily value (Figures 8–10). This approach facilitates the identification of significant seasonal patterns and anomalies [*Probst and Tardy*, 1987]. For snow storage (*SWE*) and temperature, trends were removed and daily anomalies were calculated based on the mean daily values over the modeling period (Figure 9).

Cumulative detrended runoff Q_{cd} shows the expected seasonal pattern of the hydrograph with peak runoff during summer and lowest runoff during winter (Figure 8). Differences in amplitude vary strongly between individual regions. Strongest observed temporal variability is observed between 2007 and 2009 in the western regions. In contrast, the north-eastern region shows a systematically different evolution in the time series. Here, lowest values are observed in 2008 and highest ones at the beginning and at the end of the modeling period. Variations between interannual low-flow are higher than for high-flow conditions. The strongest variation is observed between 2009 and 2011 for the majority of sites. The anomalies of the cumulative detrended runoff Q_{cda} highlight these differences in even more detail. Even though the shapes are similar, the anomalies of western and eastern sites, in particular region ID8 and ID11, show partly contrary behaviors (e.g., 2008 and 2013).

The seasonal patterns of cumulative detrended precipitation P_{cd}, and its anomalies P_{cda} are similar to the ones for Q_{cd} and Q_{cda}, respectively, but generally show a one year lag-time (Figure 8). Strongly negative Q_{cda} in 2009, for example, contrast lowest P_{cda} in 2008 for the western sites. Highest Q_{cda} in 2011 contrast highest P_{cda} in 2010. For the eastern regions this picture is not as clear and the temporal variability is more synchronous.

Anomalies of temperature T_{da} and snow stocks SWE_{da} show a distinct relationship in the summer months (Figure 9). Positive T_{da} during summer correlate with negative SWE_{da} and vice versa. The most pronounced positive T_{da} can be observed in 2008, where all sites show strong negative SWE_{da}. But even less pronounced positive T_{da}, for example in 2006, 2007, and 2011 are correlated with negative SWE_{da}. Negative summer T_{da} in 2009, 2010, and 2012 correlate with positive SWE_{da}.

The modeled cumulative *GMB* for the entire catchment is -0.52 m yr^{-1} (Figure 11) with strong differences between individual regions (Figure 10). Lowest rates between -0.34 m yr^{-1} for ID10 and -0.38 m yr^{-1} for ID9 stand in contrast to more than twofold higher rates at the westernmost regions ID8 and ID14 with -0.88 m yr^{-1} and -0.93 m yr^{-1}, respectively. *GMB* are not positive in any given year, although interannual variations are high. Only in 2009, region ID9 has an almost counterbalanced *GMB*. The detrended *GMB* shows highest variations for the westernmost regions and lowest ones for the north-eastern regions. The detrended anomalies GMB_{cda} show a similar pattern to P_{cda}, except that GMB_{cda} shows a more similar progress across individual regions. The two regions that deviate most from the mean P_{cda} pattern are ID10 and ID11. While ID11 has no glacier cover in our model, ID10 shows similar GMB_{cda} as other regions. Compared

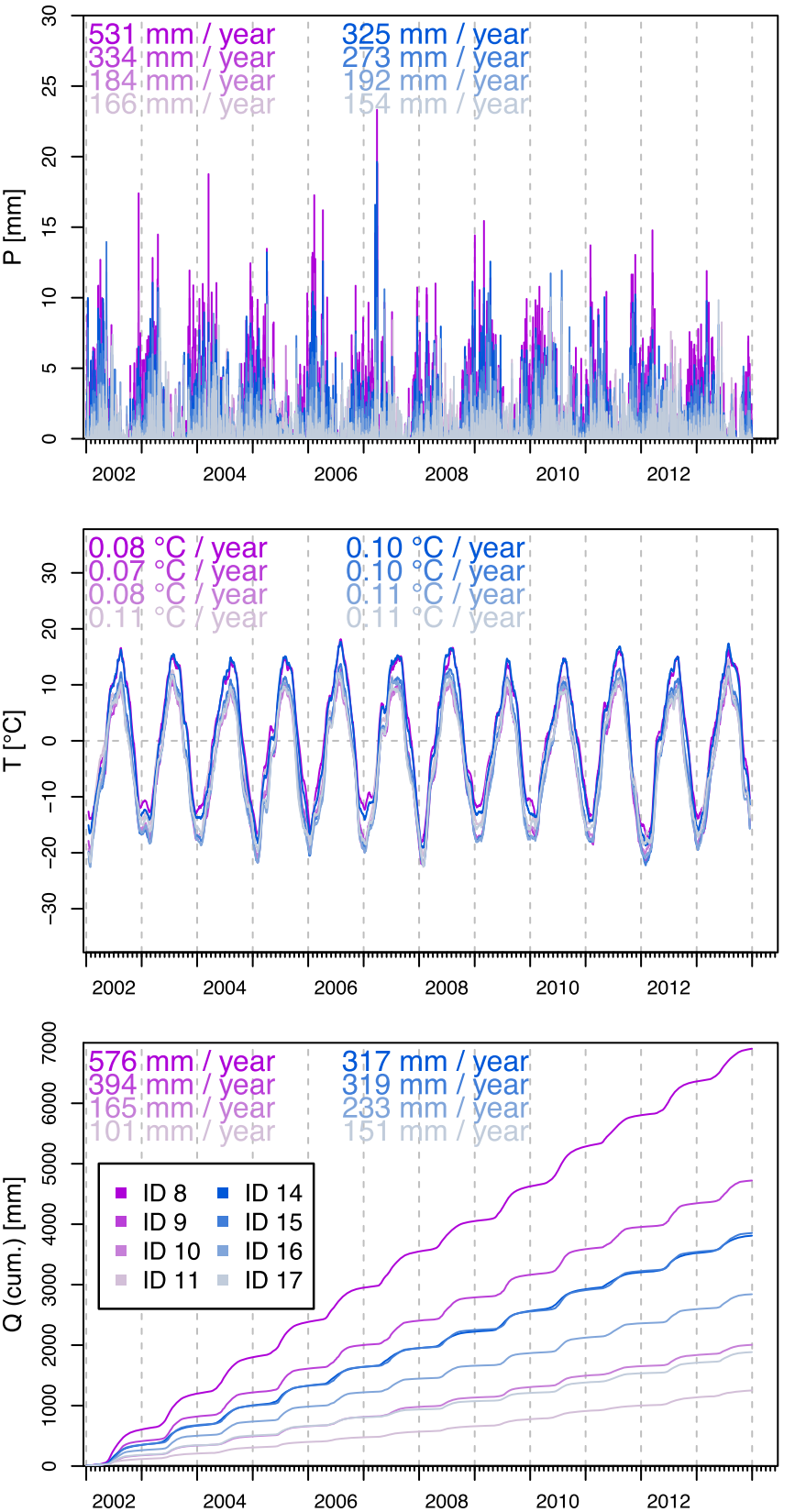

Figure 7. Time series of regional (color key) forcing parameters precipitation (*P*), temperature (*T*), and modeled cumulative total runoff (*Q*). Numbers in the top-left corners are mean annual *P*, trend in *T*, and mean annual *Q*, respectively.

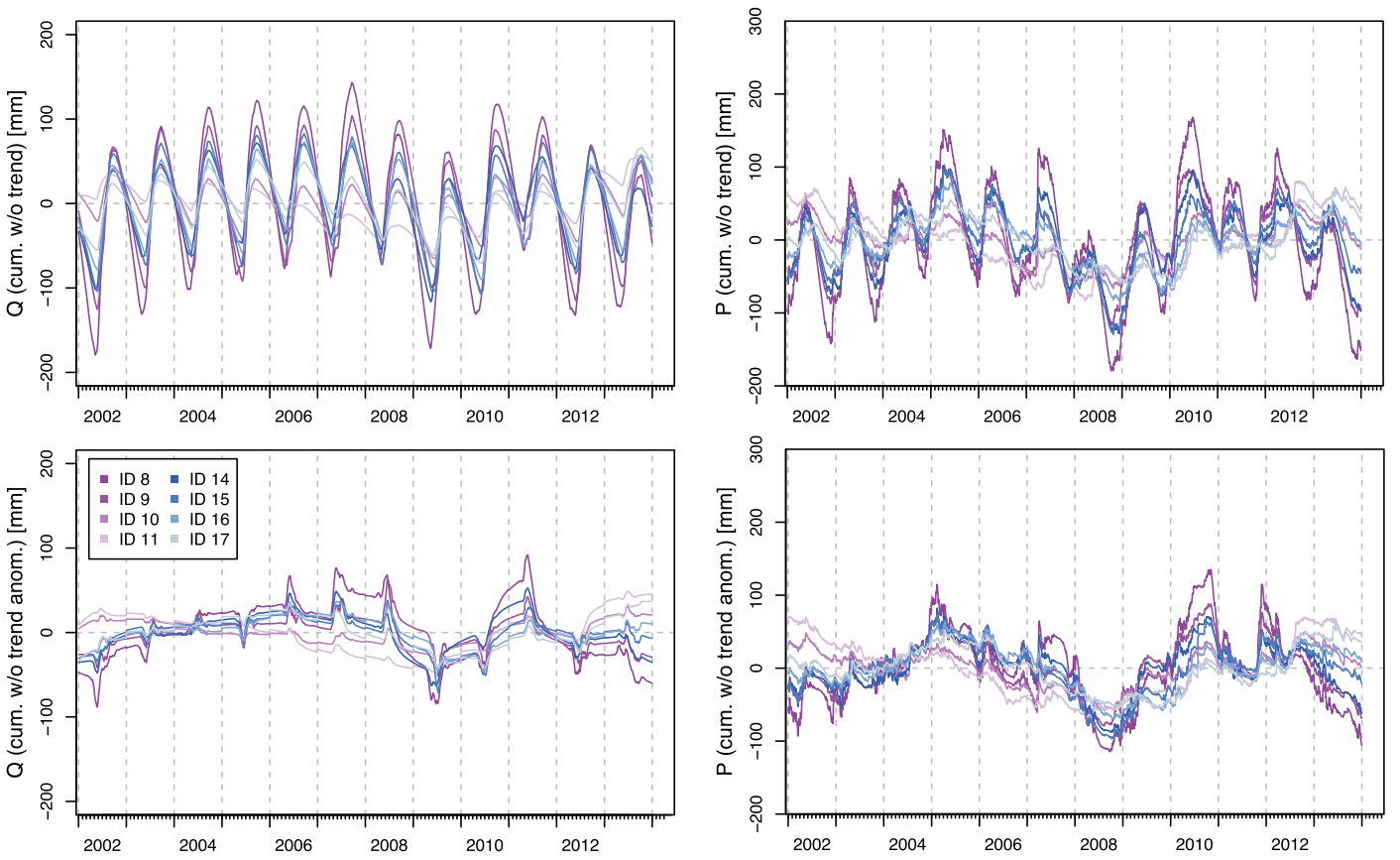

Figure 8. (top-left) Time series of regional (color key) detrended cumulative runoff Q_{cd} and (bottom-left) its daily anomalies Q_{cda}. Q_{cda} are the deviation of individual daily values of Q_{cd} from its mean value for the day of the year. (top-right) Detrended cumulative precipitation P_{cd} and (bottom-right) its anomalies P_{cda}.

to P_{cda}, GMB_{cda} shows in particular stronger negative anomalies in 2008, and overall higher variability. Negative anomalies of −300 to −200 mm and positive anomalies of 100–200 mm contrast P_{cda} anomalies of −100 mm to 100 mm with much stronger differences between individual regions.

Annual and intraannual hydrological statistics are presented in Figure 11 and summarize the modeled variability within the catchment. Strong absolute regional variability in precipitation and *GMB* during the accumulation period contrast relatively low variability in runoff components and actET at this time. This changes in summer when runoff components and actET show higher intensities and variability. While precipitation variability stays high throughout the year, *GMB* variability decreases from spring to summer. The contribution of groundwater discharge to total runoff (∼40%) strongly intensifies outside the melting period.

7. Discussion

7.1. Model Performance

The upscaled model provides a good representation of the entire catchment in terms of NSE. The additional validation for individual regions support the model but is locally difficult because of the limited in situ data records and uncertainties in the quality of these data due to the challenging political situation since Tajikistan's independence from the soviet union. The strong mismatch for recent data at site Ishkashim, but a much better fit for historic monthly means, supports this assumption. Furthermore, we assume an issue with the rating curve for high flows at site Shidz (Figure 3). This hypothesis is supported (1) by the representation of the twofold higher runoff at site Bichkarv, which underlines the good spatiotemporal representation of precipitation by the HAR data set [*Pohl et al.*, 2015b], and (2) by GRACE TWS, which do not reflect the halved amplitude of peak discharge. Gauging stations close to the Panj River are furthermore located at alluvial river channels that likely experience strong variability in river bed morphology. As the Panj marks

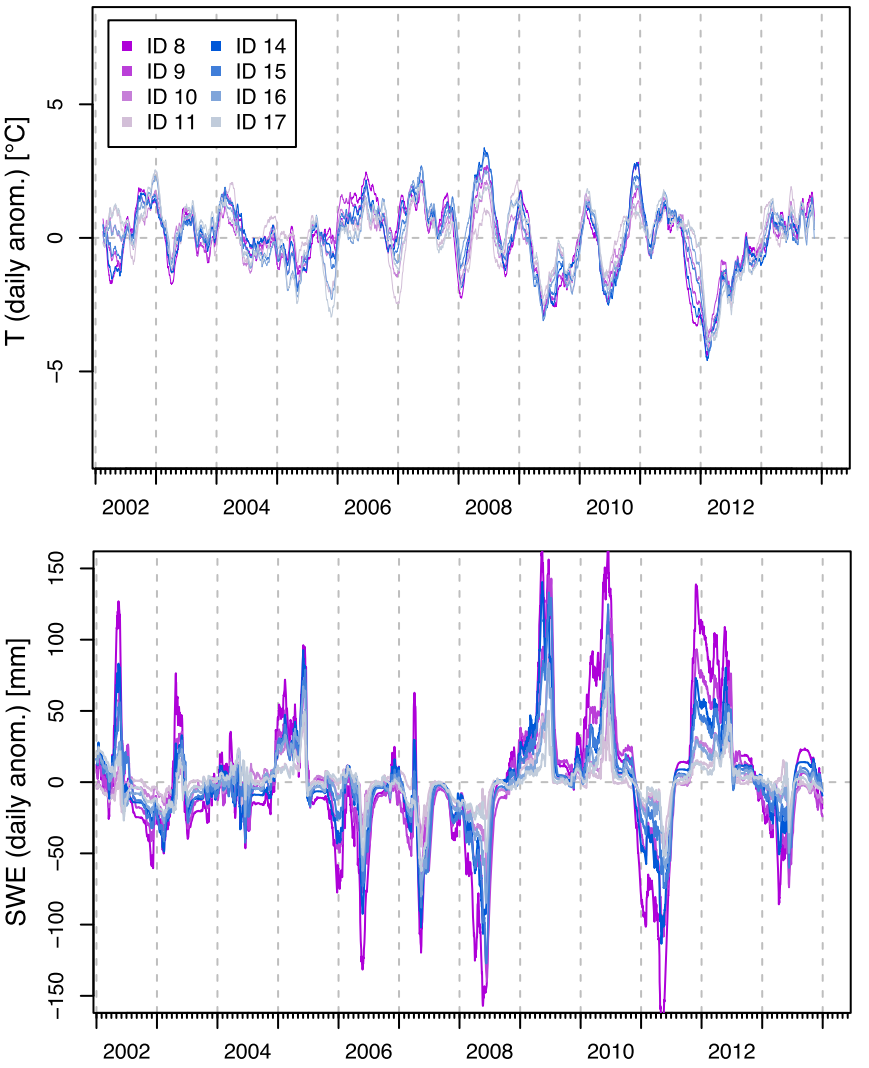

Figure 9. Time series of regional (color key) detrended temperature anomalies T_{da} and snow storage anomalies SWE_{da}. Anomalies are daily deviations from the mean value for that day of the year. Note that T_{da} is displayed as smoothed time series (30 day moving average) for visualization purposes.

the border to Afghanistan there are no recent measurements of the river channel, and discharge gauging is only based on river level measurements and rating curves.

Comparison of modeled and GRACE TWS anomalies show very similar behavior in areas where the annual TWS amplitude is high. Only in the southeastern part GRACE TWS displays much higher annual variations in TWS that contradict very low precipitation amounts of HAR and more important, in situ data [*Pohl et al.*, 2015a]. We applied the most commonly used GRACE TWS products RL05 in this study but newly developed GRACE products, or individually processed GRACE data might provide promising alternatives to more accurately reveal regional characteristics [cf. *Farinotti et al.*, 2015]. We argue that the mismatch between GRACE and modeled TWS in the southeastern part likely results from the large footprint of GRACE and resulting leakage errors, i.e., the strong amplitude in TWS of the very moist and highly glaciated Karakoram/Hindu Kush region affects the amplitude of GRACE TWS in the arid Pamir interior (ID16 and ID17) [cf. *Long et al.*, 2015]. The mixed signal consequently has a higher amplitude than the regionally modeled amplitude in TWS. Hydrological modeling such as the one we present here could be used in the future to provide better spatial constraints on gravity-based estimates, thus reducing the high local uncertainties of GRACE. Such improvements would be highly beneficial to conduct more accurate analyses of glacier mass balances [cf. *Jacob et al.*, 2012].

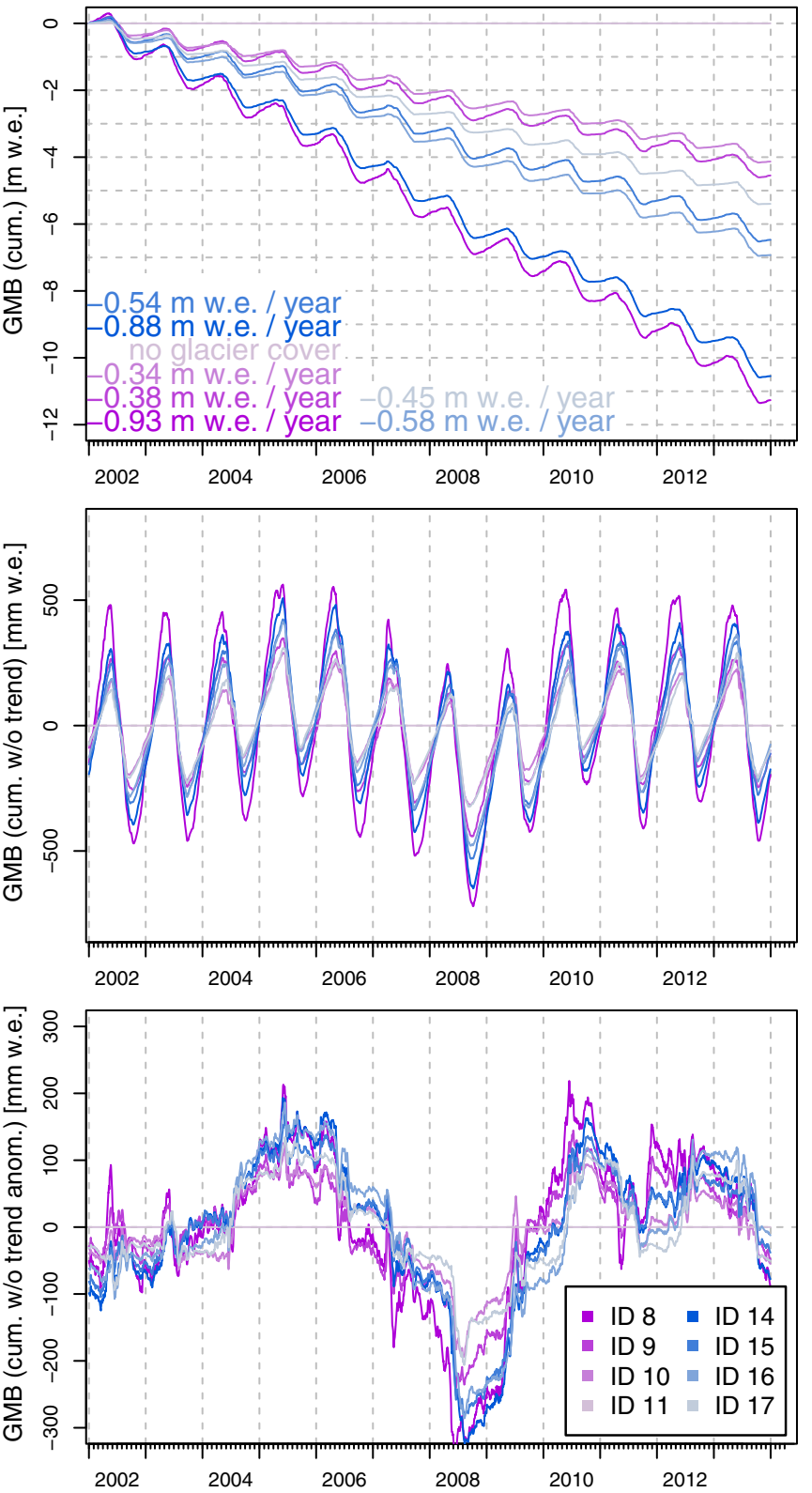

Figure 10. (top) Time series of regional (color key) cumulative glacier mass balances *GMB* with mean annual rates, (middle) detrended cumulative glacier mass balances GMB_{cd}, and (bottom) its anomalies GMB_{cda}. GMB_{cda} are daily deviations from the mean GMB_{cd} value for that day of the year. Note that the glacier cover classification shows no glaciation in the region with ID11.

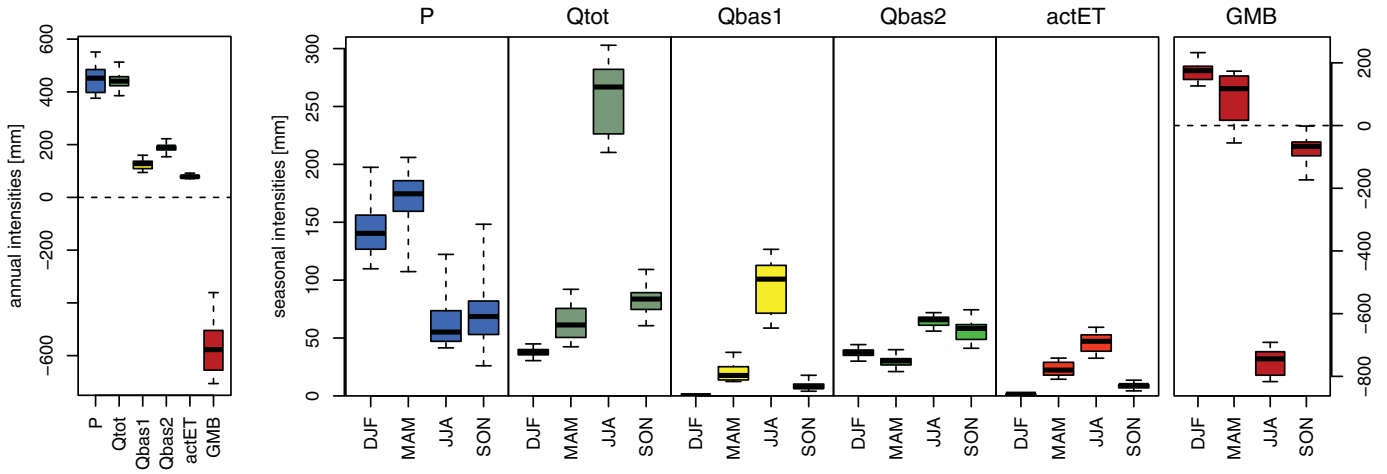

Figure 11. Annual and seasonal intensities of key hydrological components for the entire catchment area: Precipitation (P), total discharge (Qtot), fast subsurface flow resulting from snowmelt (Qbas1), groundwater (Qbas2), actual evapotranspiration (actET), and glacier mass balance (GMB). Boxplots are based on quartiles and minimum and maximum values of calculated annual or seasonal sums, respectively. Intensities for GMB are for glaciated HRUs only (11% of entire study area).

The strong linear relationship of TWS anomalies are close to the 1:1-line (Figure 5) in the winter months (NDJFMA), where precipitation falls as snow [*Immerzeel et al*., 2009; *Pohl et al*., 2015b]. It highlights the usefulness of GRACE to provide independent means to validate hydrological budgets in remote, and data scarce nival-glacial systems [*Pohl et al*., 2015b; *Werth et al*., 2009], even at regional scale. We suggest that GRACE TWS provides a unique possibility to verify the precipitation amounts provided by the data sets, and in our case to determine meaningful scaling factors. It provides an additional justification for the correction factor of 0.37 that we applied to the HAR data set. The lack of knowledge about actual amounts of precipitation in the Pamir, Hindu Kush/Karakoram region [*Palazzi et al*., 2013] demand for innovative measures. *Immerzeel et al*. [2015], for example, applied a hydrological modeling approach to show the large bias using APHRODITE data, a commonly used precipitation data set in Karakoram. In another case APHRODITE outperforms other data sets in the Central Himalayas, where enough rain gauges provide a basis for calibration and validation of such data sets [cf. *Andermann et al*., 2011]. These two examples highlight the fact that there is the need to validate the input data, for which GRACE TWS could be a good candidate. The occasional indication of a slight clock-wise hysteresis in summer (JJA) (Figure 5) could be related to a misrepresentation of evapotranspiration by the model (by the LSMs used for GRACE), which would explain the discrepancy in TWS without affecting the resulting runoff. In fact, HAR shows only marginal precipitation records in summer, but other studies have pointed out that summer recycling of evapotranspiration is an important water surplus on glaciers at the highest altitudes [*Aizen et al*., 2009]. Another explanation could be related to the modeled glacier runoff. There would be a weakening of the hysteresis if glacier runoff occurred later but was more intensive then. However, this would only be a trade-off causing a stronger mismatch between the hydrographs. The issue remains unsolved to this point, as the lack of in situ measurements for evapotranspiration, and precipitation, particularly at high altitude, prevent a more detailed analysis [cf. *Pohl et al*., 2015a].

By downscaling the temperature data to a spatial resolution of 1 × 1 km we have shown that estimated TMF_{gi} and TMF_{gs} of the original model are scale-dependent (see section 5). Corresponding parameter values for TMF_{gi} of the downscaled version are close to literature values, which are usually in the range of 7–10 mm $°C^{-1}$ d^{-1} [e.g., *Hock*, 2003]. The amounts of modeled glacier melt with the 5 × 5 km resolution are spatially consistent with reported *GMB* over the Pamir region [e.g., *Kääb et al*., 2015]. We are thus confident that the inferences concerning the amount of glacier melt from this model during the ablation season and the considerations about volumetric glacier changes presented in this paper are valid. However, the temporal distribution of melting might be biased to a small degree and the presented results should be considered as first-order estimates, subject to refinement in future studies. In addition to instrumental uncertainties in the observed discharge, and the use of coarse-gridded temperature data two other aspects

might explain the observed discrepancy in TMF_{gi}: (1) uncertainties in the derived glaciated area through MODIS MCD12Q1, and (2) unknown debris cover.

As shown in Figure 6 (section 5), the use of RGI version 5 glacier cover results in higher TMF, showing that derived TMFs are only meaningful for a particular data setup. High NSE and a good representation of observed snow cover (supporting information Figure S8) attest that obtained TMF_{gi} with our approach are meaningful for this particular setup. Inaccuracies, or inconsistencies in how glaciers are mapped, as is the case for previous RGI versions [cf. *Pohl et al*., 2015a; *Nuimura et al*., 2015], demand, in any case, for a contextual analysis of obtained values. The RGI version 5, or the newly developed but not yet publicly available GAMDAM (Glacier Area Mapping for Discharge from the Asian Mountains) [*Nuimura et al*., 2015] glacier inventory will provide superior alternatives for future modeling in the greater Pamir region. In particular, the GAMDAM inventory will provide a basis to implement effects of debris-cover to refine the hydrological conditions [*Collier et al*., 2015; *Scherler et al*., 2011b]. Debris cover, insulating glaciers, can also result in lower TMF_{gi} [*Collier et al*., 2014, 2015; *Immerzeel et al*., 2015]. In the Tian Shan only a small fraction of glaciers are debris-covered [*Farinotti et al*., 2015] (5%), but higher fractions are reported for the Karakoram [*Scherler et al*., 2011a]. A visual investigation of glaciers in the Fedchenko region but also in the southeastern part of our study area has shown insignificant debris cover on Landsat imagery. The lack of information about debris cover in currently available glacier inventories does not allow for a generic implementation of such information.

The good agreement of modeled spatial variability in *GMB* with other studies provides confidence in the approach presented here to analyze glacier melt at large scale. Less negative *GMB* towards the eastern Pamir agree well with reported glacier height changes by *Kääb et al*. [2015] based on NASA's ICESat mission data, and also with calculated specific glacier mass balances of -0.56 to -0.62 m w.e. yr^{-1}(1998–2011) reported for the Gunt catchment by *Lindner* [2013] based on geodetic methods. A recent work by *Tarasova et al*. [2016] in the Gunt catchment made use of a model calibration strategy using multicriteria objective functions, including snow cover [cf. *Finger et al*., 2015; *Duethmann et al*., 2014], and glacier mass balance [cf. *Stahl et al*., 2008; *Schaefli and Huss*, 2011] taken from *Lindner* [2013]. *Tarasova et al*. [2016] report less glacier melt contribution to total stream flow than in this study while obtaining degree-day factors for ice in the range of 10–15 mm $°C^{-1}$ d^{-1}. However, they also report a volumetric error in their modeling of at least 5.6% in the glacier mass balance. They only considered TMF_{gi} values where $TMF_{gi} > TMF_{gs}$ to account for higher albedo of snow and consequently less intensive melting of snow. With the same constraint applied to Figure 6, values for TMF_{gi} are in good agreement with those determined by *Tarasova et al*. [2016]. They also downscaled temperature and precipitation data to a spatial resolution of 1 km^2 in advance. This further indicates that the spatial resolution is the key to explain the discrepancy in obtained TMF_{gi}. Our comparison of modeled (5×5 km) and observed (MODIS) snow cover at monthly scale are in good agreement (supporting information Figure S8). This indicates that our approach provides a robust, yet simple to apply and computationally efficient way to analyze large-scale hydroclimatological dynamics. An exception are the lowermost altitude bands, where an inevitable systematic overestimation of temperatures occurs and a stronger mismatch between observed and modeled snow cover is apparent. Consequently, the model results presented here must be seen as a first-order estimate, subject to refinements if new data sets become available.

7.2. Regional Differences in Hydrology Across the Pamir

The differences in HAR precipitation and MODIS-derived glacier cover across the Pamir are reflected by the respective magnitudes in modeled runoff. However, a 5.7-fold difference in mean annual runoff between northwestern and northeastern regions contrasts an only 3.4-fold difference in mean annual precipitation (Figure 7). This difference is due to (1) the significant contributing role of glacier melt to river runoff in highly glaciated regions, and (2) the higher fraction of summer precipitation towards the east [*Pohl et al*., 2015b] that leads to higher evapotranspiration and lower runoff [*Pohl et al*., 2015a]. In the northwestern part, annual runoff exceeds the amount of annual precipitation. In the northeastern part, where no glaciation is present, 40% of the already low precipitation amounts are subject to evapotranspiration.

More runoff than annual precipitation is sustained by negative *GMB* across the Pamir. We see a continuous negative trend in *GMB* but no indication of acceleration toward the end of the period. The interannual variability is very high. Pronounced strong negative GMB_{cda} as in 2008 are, however, remediated quickly to

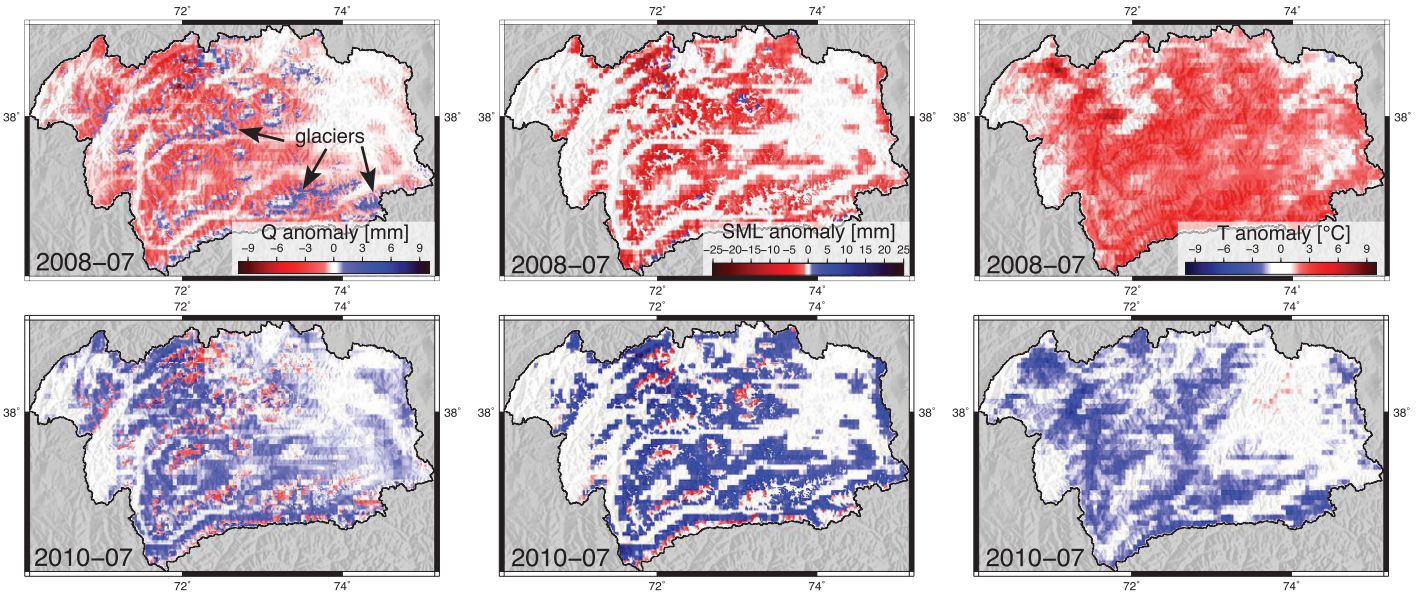

Figure 12. Hydrological conditions in summer 2008 and 2010 shown as anomalies from long-term mean conditions: (left) *Q*, (middle) snowmelt, and (right) temperature. Note the inverse *Q* anomalies with positive (negative) glacier melt and negative (positive) snowmelt anomalies.

balanced or slightly positive anomalies by 2010. The positive temperature trends of 0.07–0.12°C yr^{-1} have no noticeable effect on accelerating *GMB* trends. Interestingly, temperature trends are highest for nonglaciated regions and lowest for highly glaciated ones. This might be related to the higher amount of latent heat required for melting [*Hock*, 2005] in regions with longer lasting and more extensive snow and glacier cover. However, temperature also shows significant intraannual variability that strongly affects snow cover, snowmelt, and glacier melt. Two outstanding examples of this interaction are given in Figure 12. In the summers of 2008 and 2010, almost opposite meteorological conditions occurred. Low snow stocks due to negative precipitation and positive temperatures anomalies in 2008 (Figures 8 and 9) resulted in strong negative runoff and snowmelt anomalies for nonglaciated areas. Glacier melt, at the same time, is strongly increased and (over-) compensates the lack of snowmelt in highly glaciated regions (Figure 10, bottom).

In 2010, high precipitation and already existent snow stocks provided the main source for runoff. In combination with low temperatures, glaciers were preserved, and accordingly witnessed by negative glacier runoff anomalies (Figure 12). The "glacier compensation effect" on runoff by increased glacier melt for conditions with reduced precipitation input and vice versa [*Lang*, 1986] is apparent for high glaciation regions and appears attenuated in regions with low glacier cover (Figure 13). The compensation effect

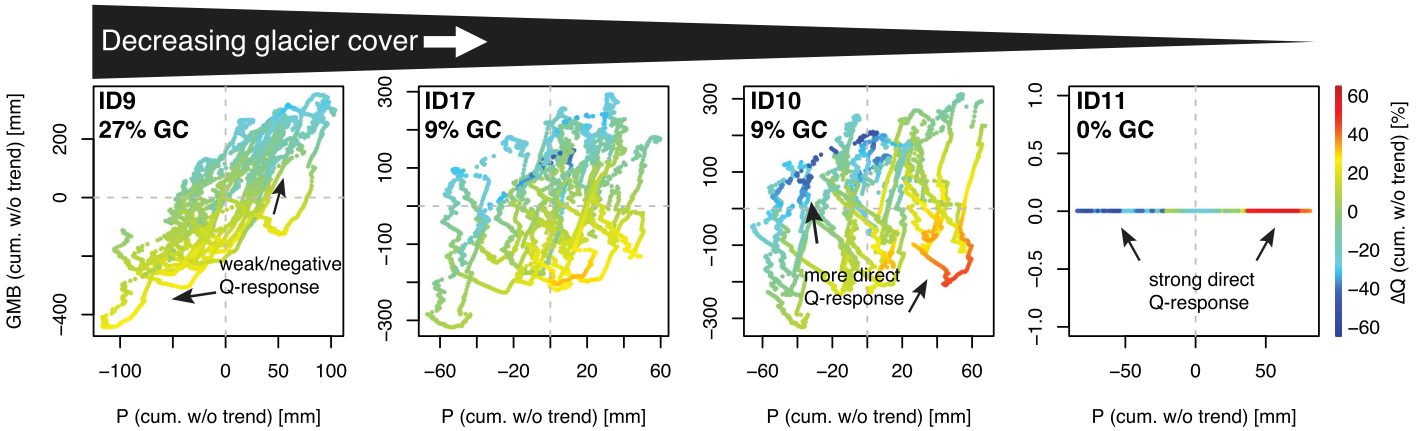

Figure 13. Effect of glaciers on stream flow buffering. Threefold dependency between runoff variability (color code) to cumulative precipitation variability and cumulative *GMB* variability with decreasing glacier cover "GC" (left to right). Note that for ID9, which encompasses the Fedchenko Glacier region, the runoff variability is anticorrelated to the other two variables.

accounts for up to 30% of runoff variability (Q_{cda}) in region ID9, contrasting up to 50% in region ID10 and ID17, and up to 60% in region ID11 with a complete lack of compensation due to no glacier cover.

The change from a negative correlation between precipitation and runoff for highly glaciated regions (Figure 13, left) into a positive correlation for low glaciated regions (Figure 13, right) corresponds to a transition from negative to positive precipitation-streamflow elasticity [cf. *Schaake and Liu*, 1987; *Andréassian et al*., 2015; *Hock et al*., 2005]. The positive correlation between precipitation and runoff is more pronounced for region ID10 compared to ID17, despite similar glacier cover. The increasing fractions of summer precipitation toward the eastern Pamir [*Pohl et al*., 2015b] (Figure 8) indicates that precipitation seasonality has a significant impact on stream flow sustainability. For the western regions, the bulk of precipitation is usually stored as snow during winter and released in the subsequent melting period, during which the groundwater storage is refilled [*Pohl et al*., 2015a]. Consequently, negative precipitation anomalies in winter result in less runoff (from groundwater discharge) in the subsequent winter. This explains the one-year offset for negative Q_{cda} compared to P_{cda} (Figure 8). It also provides an idea of how changes in precipitation distribution and lack of glacier melt buffering will change river flow variability in the western Pamir.

7.3. Runoff Sustainability

T_{da} and SWE_{da} show a strong coupling in the summer months. Positive and negative temperature anomalies trigger either melt or conservation of snow stocks. However, changes in snow cover certainly result also in a negative feedback loop with temperature due to an increased albedo, which then further affects glacier conservation [e.g., *Mölg et al*., 2013]. Based on climate model data, *Schiemann et al*. [2007] argued for a significant relation between ISM strength and Amu Darya runoff. A strong ISM causes increased troposphere temperatures that, when transferred into the Pamir, cause increased melting. Temperature anomalies certainly affect runoff but so do precipitation anomalies (Figure 12).

The presented counterbalancing of runoff by increased glacier melt during conditions when snow cover is depleted early during the year shows that such variability will also affect the evolution of glaciers. This is due to the twofold dependency on the spatiotemporal distribution of precipitation and temperature (Figure 13). Conditions, as in 2008, might occur more frequently under a warmer and more variable climate [*Intergovernmental Panel on Climate Change* (*IPCC*), 2014]. Trends in increasing temperature and shorter snow cover are already apparent in Central Asia [*Dietz et al*., 2014; *Aizen et al*., 1997; *Makhmadaliev et al*., 2008].

To assess future hydrology, *Kure et al*. [2013b] have applied climate models and analyzed climate change scenarios to predict an even stronger increase in temperature until 2100 of 4–5°C. At the same time, precipitation amounts were predicted to either show no or a mere increase by 7% at the most, which would unlikely compensate for increased ablation [cf. *Oerlemans and Fortuin*, 1992]. Such conditions would favor situations like in 2008 and would imply increasing glacier retreat in the future. These predictions are different than for the Karakoram. *Kapnick et al*. [2014] showed that increasing precipitation actually overcompensates an increase in temperature, resulting in more snow cover. *Kure et al*. [2013a] derived a shift in the seasonality of runoff for Pamir rivers toward sooner onset of melting and significantly reduced runoff toward the end of summer, given much earlier depletion of snow cover and a reduction in glacier cover. Higher river runoff variability due to the lack of glacier melt buffering might affect the natural threshold of resilience to water availability [*Nolin*, 2012]. This effect might be enhanced because most precipitation is currently being received in spring as snow (Figure 11). A warmer climate implies changes in precipitation phase at this time, exerting even more variability on spring *GMB*. Glacier accumulation types in the Karakoram have been described as intermediate summer-winter-types due to the influence of midlatitude westerlies and the Indian summer monsoon [*Hewitt*, 2011], highlighting the vulnerability of sustainable river flow to increasing air temperatures.

Earlier and reduced snowmelt will also affect winter runoff because snowmelt is the main source for groundwater recharge [*Pohl et al*., 2015a] (Figure 11). The importance of groundwater discharge to the annual total runoff (~40%) is not surprising [*Andermann et al*., 2012; *Jasechko et al*., 2016] but water reservoirs in the Pamir built mainly for hydropower will have to adapt to changing seasonalities and the sooner attenuation of groundwater discharge. This will also affect water availability in downstream regions and might be intensified due to increased evapotranspiration (cf. Figure 11), and the resulting decrease in net precipitation contribution to river runoff. Such conditions would result when higher fractions of precipitation are received as rain during single events [*Pohl et al*., 2015a]. The ratio of precipitation to runoff is

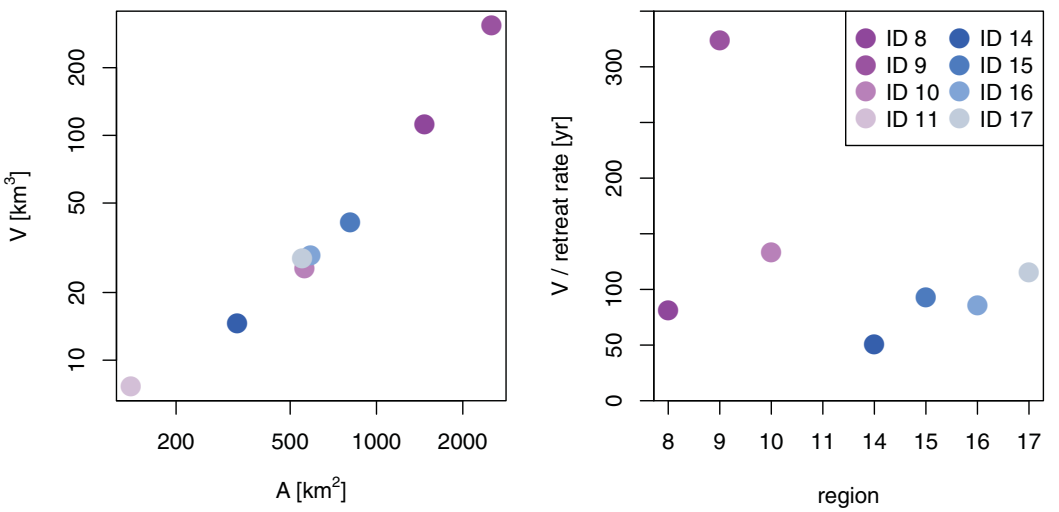

Figure 14. Calculated glacier mass volumes based on information taken from the Randolph Glacier Inventory (RGI) version 5 [*Arendt et al.*, 2015] and equations after *Grinsted* [2013] (left), and resulting disappearance time assuming constant rates and uniform glacier distribution (right). Region ID11 has no calculated value because no glaciers are present in the actual study area according to the land cover classification used.

highest for little-glaciated and high summer-fraction precipitation regions (Figure 7). Under climate warming, this ratio might be further enhanced, applying additional pressure to Central Asia's rapidly growing population (1.5% yr^{-1}; *United Nations Department of Economic and Social Affairs* [2015]). The cultivation of water-intensive but low cost-efficient crops, such as cotton and wheat [*Thenkabail and Wu*, 2012; *Varis*, 2014] add to the conflict potential, demanding for new management strategies [*Bernauer and Siegfried*, 2012; *Gleick and Heberger*, 2014].

Threefold stronger negative *GMB* calculated for the westernmost region compared to the eastern regions highlight strong spatial variability (Figure 10). Values between -0.34 and -0.54 m yr^{-1} for the central and eastern regions are in good agreement with calculations by *Kääb et al.* [2015], who have reported glacier height changes of -0.48 ± 0.14 m yr^{-1} for the Pamir domain based on laser altimetry during the period 2003–2008. As shown in Figure 10, 2008 shows particularly large negative anomalies, which might indicate that these values contribute to slightly overestimate a long-term trend. The complex interactions of meteorological parameters impede precise predictions of glacier and river runoff evolution. Using glacier extents from the RGI version 5, we calculated glacier volumes for individually analyzed regions after *Grinsted* [2013] (supporting information S4). The resulting volumes and times until volume depletion under the assumption of uniform ablation are shown in Figure 14. We are aware that ablation is not uniform at the elevation ranges [e.g., *Barrand et al.*, 2010; *Huss et al.*, 2008], and hence glacier retreat to higher elevations toward steady state conditions is not reflected in this estimate. Neither are the model uncertainties reflected in this estimate that result from the chosen approach with the coarse temperature data. However, this rough estimation provides a first relationship of how the modeled and observed *GMB* in the region correspond to current glacier volumes. Even with a nonaccelerated trend in warming, significant changes in glacier volume would be expected for most parts of Pamir toward the end of this and the beginning of the next century. Region ID9, encompassing the Fedchenko region, shows much longer resistance times, but a shift toward more rainfall, higher temperatures, and resulting less snow cover might affect these results due to the missing reflective and protecting properties of the snow cover [*Mölg et al.*, 2013].

The reported slight mass gain for glaciers in the Karakoram and eastern Pamir [*Gardelle et al.*, 2013; *Kääb et al.*, 2015] located outside the study area reflects the trend toward less negative *GMB* trends in the east. It should also be noted that the simulated *GMB* represent the mean of all HRUs that were classified as glacier covered. Calculations by *Gardelle et al.* [2013] do not consider the entirety of glacier area. In fact, *GMB* are much more negative for lower elevations in the present study. Especially the small glaciers in the western part of the Pamir show lower altitudes compared to more eastern regions, reflected by the precipitation gradients from the margins towards the Pamir's interior. Glaciers in the Karakoram and eastern Pamir with

reported positive *GMB* [*Gardelle et al*., 2013; *Kääb et al*., 2015] are located in more summer-precipitation influenced regions [*Pohl et al*., 2015b] and their associated intermediate winter-/summer-type glacier accumulation [*Hewitt*, 2011]. The strong difference in west-east direction might therefore be attributed to the different moisture supply regimes, providing the critical boundary conditions for long-term glacier evolution [*Mölg et al*., 2013].

Regardless of the hydrological components addressed in the present study, the apparent positive temperature trend exerts the danger of more frequent natural hazards. *Mergili et al*. [2012] has outlined the large areas that will be affected by a change in the permafrost boundary. The forming of periglacial lakes increases the chance of GLOFs, and thawing permafrost as well as higher portions of rainfall over snowfall increases the chance of landslides and mudflows [*Gruber and Mergili*, 2013].

8. Conclusions

We successfully upscaled a hydrological model previously applied and calibrated for a catchment in the central Pamir. The upscaled model for the Panj River catchment permits assessment of large-scale dynamics of the entire drainage system of the Pamir. A NSE of 0.87 for the entire catchment and the ability of the model to resolve regional differences suggest that meteorological forcing parameters and the chosen approach represent a good choice for this data scarce and complex region of the world. A comparison of the model outputs with GRACE TWS anomalies shows good agreement for most regions but witnesses much higher amplitudes in the GRACE signal in the arid southeastern part. We attribute this deviation to much higher amplitudes of mass variations in the Karakoram that leads to leakage errors in the eastern Pamir. This consequently reduces the ability of GRACE data to resolve the spatially very heterogenous system. Despite local differences in amplitude, TWS anomalies of GRACE, and from the hydrological model show a strong linear relationship in the winter months. This validates the good representation of the spatiotemporal precipitation patterns of the HAR data set, and exemplifies the strong potential of GRACE for validating precipitation data sets in snowfall-dominated catchments even at regional scale. Uncertainties in the modeling result from the use of the large gridded temperature data set that simplifies melting processes but favors ease of use and computational expense. Consequently, the good agreement between modeled snow cover and estimates from MODIS decreases where a finer spatial resolution would be needed to precisely resolve local melting processes. Therefore, results presented in this study for the greater Pamir region have to be seen as first-order estimates that might certainly be improved with a finer forcing in the future.

Annual precipitation amounts show up to 3.4-fold regional differences, contrasting up to 5.7-fold differences in observed river runoff. These differences are explained by (1) negative glacier mass balances that contribute significantly to annual runoff and (2) the change in seasonal precipitation distribution with more summer rainfall and resulting higher evapotranspiration towards the east. Variability in climatic forcing on the resulting river runoff is buffered by the glaciers. Low precipitation can be compensated for by glacier melts but this feature is at stake due to shrinking glaciated areas. In strongly glaciated areas a negative feedback between precipitation and runoff is observable, and only 30% of the amplitude in precipitation variability is reflected by runoff variability. In contrast, precipitation variability accounts for up to up to 60% of runoff variability in low or nonglaciated regions. Higher precipitation and glaciation in the western parts result here in a contribution of more than 70% of the total discharge by snow and ice melt from glaciated areas.

All regions experience continuous, negative glacier mass balances over the study period (average: -0.52 m yr^{-1}). This phenomenon is more pronounced in the western part of the Pamir. However, the snow accumulation during winter, and summer temperature anomalies contribute to strong annual differences. A robust trend in the time series, complementing other studies in the greater Pamir region, facilitates a first-order estimation of glacier diminution rates. It implies that, with the exception of the region around the Fedchenko Glacier, and even with no significant increase in temperatures due to global warming, severe changes in the sustainability of river flow might be expected towards the end of this century. Therefore, water and agricultural management in Central Asia would need to adapt to mitigate rising conflict potentials at trans-boundary and subnational levels.

Acknowledgments
This work is part of the BMBF (Federal Ministry of Education and Research) research program PAMIR (FKZ 03G0815) within the CAME project (Central Asia and Tibet: Monsoon dynamics and geo-ecosystems) and funded by the BMBF. MODIS MOD11C1 and MCD12Q1 data are distributed by the Land Processes Distributed Active Archive Center (LP DAAC), located at the US Geological Survey (USGS) Earth Resources Observation and Science (EROS) Center (lpdaac.usgs.gov). GRACE land is available at http://grace.jpl.nasa.gov, supported by the NASA MEaSUREs Program. We thank the State Administration for Hydrometeorology of Tajikistan for their cooperation and providing the discharge data. We would like to thank the editor, Laurent Longuevergne and two anonymous reviewers for their comments and suggestions that greatly helped to improved this manuscript. The PAMIR team further includes Christiane Meier, Stephan Weise, Karsten Osenbrück, Stefan Geyer, Tino Rödiger, Christian Siebert, and Wolfgang Busch.

References

Aizen, V. B., E. M. Aizen, J. M. Melack, and J. Dozier (1997), Climatic and hydrologic changes in the Tien Shan, Central Asia, *J. Clim.*, *10*(6), 1393–1404, doi:10.1175/1520-0442(1997)010 < 1393:CAHCIT>2.0.CO;2.

Aizen, V. B., P. A. Mayewski, E. M. Aizen, D. R. Joswiak, A. B. Surazakov, S. Kaspari, B. Grigholm, M. Krachler, M. Handley, and A. Finaev (2009), Stable-isotope and trace element time series from Fedchenko glacier (Pamirs) snow/firn cores, *J. Glaciol.*, *55*(190), 275–291, doi:10.3189/002214309788608787.

Allen, R. G., L. S. Pereira, D. Raes, and M. Smith (1998), *Crop Evapotranspiration—Guidelines for Computing Crop Water Requirements*, 56 ed., 290 pp., Food Agric. Organ. of the U. N., Rome.

An, Z., et al. (2012), Interplay between the Westerlies and Asian monsoon recorded in Lake Qinghai sediments since 32 ka, *Sci. Rep.*, *2*, 619, doi:10.1038/srep00619.

Andermann, C., S. Bonnet, and R. Gloaguen (2011), Evaluation of precipitation data sets along the Himalayan front, *Geochem. Geophys. Geosyst.*, *12*, Q07023, doi:10.1029/2011GC003513.

Andermann, C., A. Crave, R. Gloaguen, P. Davy, and S. Bonnet (2012), Connecting source and transport: Suspended sediments in the Nepal Himalayas, *Earth Planet. Sci. Lett.*, *351–352*, 158–170, doi:10.1016/j.epsl.2012.06.059.

Andréassian, V., L. Coron, J. Lerat, and N. Le Moine (2015), Climate elasticity of streamflow revisited—An elasticity index based on long-term hydrometeorological records, *Hydrol. Earth Syst. Sci. Discuss.*, *12*(4), 3645–3679, doi:10.5194/hessd-12-3645-2015.

Arendt, A., et al. (2015), Randolph Glacier Inventory—A Dataset of Global Glacier Outlines: Version 5.0 [Digital Media], Global Land Ice Measur. from Space, Boulder Colo.

Barrand, N. E., T. D. James, and T. Murray (2010), Spatio-temporal variability in elevation changes of two high-Arctic valley glaciers, *J. Glaciol.*, *56*(199), 771–780, doi:10.3189/002214310794457362.

Bernauer, T., and T. Siegfried (2012), Climate change and international water conflict in Central Asia, *J. Peace Res.*, *49*(1), 227–239, doi:10.1177/0022343311425843.

Bhatta, G., P. Aggarwal, S. Poudel, and D. Belgrave (2015), Climate-induced migration in South Asia: Migration decisions and gender dimensions of adverse climatic events, *J. Rural Community Dev.*, *10*(4), 1–23.

Biskop, S., F. Maussion, P. Krause, and M. Fink (2016), Differences in the water-balance components of four lakes in the southern-central Tibetan Plateau, *Hydrol. Earth Syst. Sci.*, *20*(1), 209–225, doi:10.5194/hess-20-209-2016.

Bolch, T., et al. (2012), The state and fate of Himalayan glaciers, *Science*, *336*(6079), 310–314, doi:10.1126/science.1215828.

Chiew, F. H. S. (2006), Estimation of rainfall elasticity of streamflow in Australia, *Hydrol. Sci. J.*, *51*(4), 613–625, doi:10.1623/hysj.51.4.613.

Collier, E., L. I. Nicholson, B. W. Brock, F. Maussion, R. Essery, and A. B. G. Bush (2014), Representing moisture fluxes and phase changes in glacier debris cover using a reservoir approach, *The Cryosphere*, *8*(4), 1429–1444, doi:10.5194/tc-8-1429-2014.

Collier, E., F. Maussion, L. I. Nicholson, T. Mölg, W. W. Immerzeel, and A. B. G. Bush (2015), Impact of debris cover on glacier ablation and atmosphere-glacier feedbacks in the Karakoram, *The Cryosphere*, *9*(4), 1617–1632, doi:10.5194/tc-9-1617-2015.

Curio, J., F. Maussion, and D. Scherer (2015), A 12-year high-resolution climatology of atmospheric water transport over the Tibetan Plateau, *Earth Syst. Dyn.*, *6*(1), 109–124, doi:10.5194/esd-6-109-2015.

Dee, D. P., et al. (2011), The ERA-Interim reanalysis: Configuration and performance of the data assimilation system, *Q. J. R. Meteorol. Soc.*, *137*(656), 553–597, doi:10.1002/qj.828.

Dietz, A., C. Conrad, C. Kuenzer, G. Gesell, and S. Dech (2014), Identifying changing snow cover characteristics in Central Asia between 1986 and 2014 from Remote Sensing Data, *Remote Sens.*, *6*(12), 12,752–12,775, doi:10.3390/rs61212752.

Duethmann, D., J. Zimmer, A. Gafurov, A. Güntner, D. Kriegel, B. Merz, and S. Vorogushyn (2013), Using hydrological modelling for the evaluation of areal precipitation estimates based on downscaled reanalysis and station data in data sparse mountainous catchments in Central Asia, *Geophys. Res. Abstr.*, *15*, EGU2013-7511-1.

Duethmann, D., J. Peters, T. Blume, S. Vorogushyn, and A. Güntner (2014), The value of satellite-derived snow cover images for calibrating a hydrological model in snow-dominated catchments in Central Asia, *Water Resour. Res.*, *50*, 2002–2021, doi:10.1002/2013WR014382.

FAO, IIASA, ISRIC, ISSCAS, and JRC (2009), *Harmonized World Soil Database (version 1.1)*, Rome, Italy.

Farinotti, D., L. Longuevergne, G. Moholdt, D. Duethmann, T. Mölg, T. Bolch, S. Vorogushyn, and A. Güntner (2015), Substantial glacier mass loss in the Tien Shan over the past 50 years, *Nat. Geosci.*, *8*(9), 716–722, doi:10.1038/ngeo2513.

Feng, W., M. Zhong, J.-M. Lemoine, R. Biancale, H.-T. Hsu, and J. Xia (2013), Evaluation of groundwater depletion in North China using the Gravity Recovery and Climate Experiment (GRACE) data and ground-based measurements, *Water Resour. Res.*, *49*, 2110–2118, doi:10.1002/wrcr.20192.

Finger, D., M. Vis, M. Huss, and J. Seibert (2015), The value of multiple data set calibration versus model complexity for improving the performance of hydrological models in mountain catchments, *Water Resour. Res.*, *51*, 1939–1958, doi:10.1002/2014WR015712.

Fuchs, M. C., R. Gloaguen, and E. Pohl (2013), Tectonic and climatic forcing on the Panj river system during the Quaternary, *Int. J. Earth Sci.*, *102*(7), 1985–2003, doi:10.1007/s00531-013-0916-2.

Fuchs, M. C., R. Gloaguen, S. Merchel, E. Pohl, V. A. Sulaymonova, C. Andermann, and G. Rugel (2015), Denudation rates across the Pamir based on 10Be concentrations in fluvial sediments: Dominance of topographic over climatic factors, *Earth Surf. Dyn.*, *3*(3), 423–439, doi:10.5194/esurf-3-423-2015.

Gardelle, J., E. Berthier, Y. Arnaud, and A. Kääb (2013), Region-wide glacier mass balances over the Pamir-Karakoram-Himalaya during 1999–2011, *The Cryosphere*, *7*(4), 1263–1286, doi:10.5194/tc-7-1263-2013.

Gardner, A. S., et al. (2013), A reconciled estimate of glacier contributions to sea level rise: 2003 to 2009, *Science*, *340*(6134), 852–857, doi:10.1126/science.1234532.

Gleick, P. H., and M. Heberger (2014), *The World's Water*, 173–219 pp., Island Press/Cent. for Resour. Econ., Washington, D. C., doi:10.5822/978-1-61091-483-3.

Grinsted, A. (2013), An estimate of global glacier volume, *The Cryosphere*, *7*(1), 141–151, doi:10.5194/tc-7-141-2013.

Gruber, F. E., and M. Mergili (2013), Regional-scale analysis of high-mountain multi-hazard and risk indicators in the Pamir (Tajikistan) with GRASS GIS, *Nat. Hazards Earth Syst. Sci.*, *13*(11), 2779–2796, doi:10.5194/nhess-13-2779-2013.

Güntner, A., J. Stuck, S. Werth, P. Döll, K. Verzano, and B. Merz (2007), A global analysis of temporal and spatial variations in continental water storage, *Water Resour. Res.*, *43*, W05416, doi:10.1029/2006WR005247.

Hagg, W., M. Hoelzle, S. Wagner, E. Mayr, and Z. Klose (2013), Glacier and runoff changes in the Rukhk catchment, upper Amu-Darya basin until 2050, *Global Planet. Change*, *110*, 62–73, doi:10.1016/j.gloplacha.2013.05.005.

Hall, D. K., V. V. Salomonson, and G. A. Riggs (2006), *MODIS/Terra Snow Cover Monthly L3 Global 0.05Deg CMG V005*, Natl. Snow and Ice Data Cent., Boulder, Colo.

Hewitt, K. (2011), Glacier change, concentration, and elevation effects in the Karakoram Himalaya, Upper Indus Basin, *Mt. Res. Dev.*, *31*(3), 188–200, doi:10.1659/MRD-JOURNAL-D-11-00020.1.

Hock, R. (2003), Temperature index melt modelling in mountain areas, *J. Hydrol.*, *282*(1–4), 104–115, doi:10.1016/S0022-1694(03)00257-9.

Hock, R. (2005), Glacier melt: A review of processes and their modelling, *Prog. Phys. Geogr.*, *29*(3), 362–391, doi:10.1191/0309133305pp453ra.

Hock, R., P. Jansson, and L. N. Braun (2005), Modelling the response of mountain glacier discharge to climate warming, in *Global Change and Mountain Regions*, edited by U. M. Huber, H. K. M. Bugmann, and M. A. Reasoner, pp. 243–252, Springer, Netherlands, doi:10.1007/1-4020-3508-X_25.

Huss, M., A. Bauder, M. Funk, and R. Hock (2008), Determination of the seasonal mass balance of four Alpine glaciers since 1865, *J. Geophys. Res.*, *113*, F01015, doi:10.1029/2007JF000803.

Immerzeel, W., P. Droogers, S. de Jong, and M. Bierkens (2009), Large-scale monitoring of snow cover and runoff simulation in Himalayan river basins using remote sensing, *Remote Sensing of Environment*, *113*(1), 40–49, doi:10.1016/j.rse.2008.08.010.

Immerzeel, W. W., L. P. H. van Beek, and M. F. P. Bierkens (2010), Climate change will affect the Asian water towers, *Science*, *328*(5984), 1382–5, doi:10.1126/science.1183188.

Immerzeel, W. W., N. Wanders, A. F. Lutz, J. M. Shea, and M. F. P. Bierkens (2015), Reconciling high-altitude precipitation in the upper Indus basin with glacier mass balances and runoff, *Hydrol. Earth Syst. Sci.*, *19*(11), 4673–4687, doi:10.5194/hess-19-4673-2015.

Intergovernmental Panel on Climate Change (IPCC) (2014), *Climate Change 2014: Synthesis Report. Contribution of Working Groups I, II and III to the Fifth Assessment Report of the Intergovernmental Panel on Climate Change*, 151 pp., IPCC, Geneva, Switzerland.

Jacob, T., J. Wahr, W. T. Pfeffer, and S. Swenson (2012), Recent contributions of glaciers and ice caps to sea level rise, *Nature*, *482*(7386), 514–518, doi:10.1038/nature10847.

Jasechko, S., J. W. Kirchner, J. M. Welker, and J. J. McDonnell (2016), Substantial proportion of global streamflow less than three months old, *Nat. Geosci.*, *9*(2), 126–129, doi:10.1038/ngeo2636.

Kääb, A., D. Treichler, C. Nuth, and E. Berthier (2015), Brief Communication: Contending estimates of 2003–2008 glacier mass balance over the Pamir-Karakoram-Himalaya, *The Cryosphere*, *9*(2), 557–564, doi:10.5194/tc-9-557-2015.

Kapnick, S. B., T. L. Delworth, M. Ashfaq, S. Malyshev, and P. C. D. Milly (2014), Snowfall less sensitive to warming in Karakoram than in Himalayas due to a unique seasonal cycle, *Nat. Geosci.*, *7*(11), 834–840, doi:10.1038/ngeo2269.

Khromova, T., G. Osipova, D. Tsvetkov, M. Dyurgerov, and R. Barry (2006), Changes in glacier extent in the eastern Pamir, Central Asia, determined from historical data and ASTER imagery, *Remote Sens. Environ.*, *102*(1–2), 24–32, doi:10.1016/j.rse.2006.01.019.

Kralisch, S., P. Krause, M. Fink, C. Fischer, and W. Flügel (2007), Component based environmental modelling using the JAMS framework, in *Proceedings of MODSIM07*, edited by L. Oxley and D. Kulasiri, pp. 812–818, Modell. and Simul. Soc. of Australia and New Zealand, Christchurch, New Zealand.

Krause, P., and S. Hanisch (2009), Simulation and analysis of the impact of projected climate change on the spatially distributed waterbalance in Thuringia, Germany, *Adv. Geosci.*, *21*, 33–48, doi:10.5194/adgeo-21-33-2009.

Kure, S., S. Jang, N. Ohara, M. L. Kavvas, and Z. Q. Chen (2013a), Hydrologic impact of regional climate change for the snowfed and glacierfed river basins in the Republic of Tajikistan: Hydrological response of flow to climate change, *Hydrol. Processes*, *27*(26), 4057–4070, doi:10.1002/hyp.9535.

Kure, S., S. Jang, N. Ohara, M. L. Kavvas, and Z. Q. Chen (2013b), Hydrologic impact of regional climate change for the snow-fed and glacier-fed river basins in the Republic of Tajikistan: Statistical downscaling of global climate model projections, *Hydrol. Processes*, *27*(26), 4071–4090, doi:10.1002/hyp.9536.

Landerer, F. W., and S. C. Swenson (2012), Accuracy of scaled GRACE terrestrial water storage estimates, *Water Resour. Res.*, *48*, W04531, doi:10.1029/2011WR011453.

Lang, H. (1986), Forecasting meltwater runoff from snow-covered areas and from glacier basins, in *River Flow Modelling and Forecasting SE-5, Water Science and Technology Library*, vol. 3, edited by D. A. Kraijenhoff and J. R. Moll, pp. 99–127, Springer, Netherlands, doi:10.1007/978-94-009-4536-4_5.

Lindner, M. I. f. G. I. (2013), Rezente Gletscheränderung im Einzugsgebiet des Gunts (Tadschikistan) [GER], Master thesis, Universität Innsbruck, Innsbruck.

Liu, X., U. Herzschuh, Y. Wang, G. Kuhn, and Z. Yu (2014), Glacier fluctuations of Muztagh Ata and temperature changes during the late Holocene in westernmost Tibetan Plateau, based on glaciolacustrine sediment records, *Geophys. Res. Lett.*, *41*, 6265–6273, doi:10.1002/2014GL060444.

Long, D., L. Longuevergne, and B. R. Scanlon (2015), Global analysis of approaches for deriving total water storage changes from GRACE satellites, *Water Resour. Res.*, *51*, 2574–2594, doi:10.1002/2014WR016853.

Lutz, A. F., W. W. Immerzeel, A. Gobiet, F. Pellicciotti, and M. F. P. Bierkens (2013), Comparison of climate change signals in CMIP3 and CMIP5 multi-model ensembles and implications for Central Asian glaciers, *Hydrol. Earth Syst. Sci.*, *17*(9), 3661–3677, doi:10.5194/hess-17-3661-2013.

Lutz, A. F., W. W. Immerzeel, A. B. Shrestha, and M. F. P. Bierkens (2014), Consistent increase in High Asia's runoff due to increasing glacier melt and precipitation, *Nat. Clim. Change*, *4*(7), 587–592, doi:10.1038/nclimate2237.

Makhmadaliev, B., A. Kayumov, V. Novikov, N. Mustaeva, and I. Rajabov (2008), The Second National Communication of the Republic of Tajikistan under the United Nations framework convention on climate change, technical report, State Agency for Hydrometeorol., Dushanbe, Tajikistan. [Available at http://unfccc.int/resource/docs/natc/tainc2.pdf.]

Maussion, F., D. Scherer, R. Finkelnburg, J. Richters, W. Yang, and T. Yao (2011), WRF simulation of a precipitation event over the Tibetan Plateau, China—An assessment using remote sensing and ground observations, *Hydrol. Earth Syst. Sci.*, *15*(6), 1795–1817, doi:10.5194/hess-15-1795-2011.

Maussion, F., D. Scherer, T. Mölg, E. Collier, J. Curio, and R. Finkelnburg (2014), Precipitation seasonality and variability over the Tibetan Plateau as resolved by the high Asia reanalysis, *J. Clim.*, *27*(5), 1910–1927, doi:10.1175/JCLI-D-13-00282.1.

Mergili, M., C. Kopf, B. Müllebner, and J. F. Schneider (2012), Changes of the cryosphere and related geohazards in the high-mountain areas of Tajikistan and Austria: A Comparison, *Geogr. Ann. Ser. A*, *94*(1), 79–96, doi:10.1111/j.1468-0459.2011.00450.x.

Mölg, T., F. Maussion, W. Yang, and D. Scherer (2012), The footprint of Asian monsoon dynamics in the mass and energy balance of a Tibetan glacier, *The Cryosphere*, *6*(6), 1445–1461, doi:10.5194/tc-6-1445-2012.

Mölg, T., F. Maussion, and D. Scherer (2013), Mid-latitude westerlies as a driver of glacier variability in monsoonal High Asia, *Nat. Clim. Change*, *4*(1), 68–73, doi:10.1038/nclimate2055.

Nash, J., and J. Sutcliffe (1970), River flow forecasting through conceptual models. Part I—A discussion of principles, *J. Hydrol.*, *10*(3), 282–290, doi:10.1016/0022-1694(70)90255-6.
National Centers for Environmental Prediction NOAA, U.S. Department of Commerce, N. W. S. (2000), NCEP FNL Operational Model Global Tropospheric Analyses, continuing from July 1999, doi:10.5065/D6M043C6.
Nolin, A. W. (2012), Perspectives on climate change, Mountain hydrology, and water resources in the Oregon Cascades, USA, *Mt. Res. Dev.*, *32*(S1), S35–S46, doi:10.1659/MRD-JOURNAL-D-11-00038.S1.
Nuimura, T., et al. (2015), The GAMDAM glacier inventory: A quality-controlled inventory of Asian glaciers, *The Cryosphere*, *9*(3), 849–864, doi:10.5194/tc-9-849-2015.
Oerlemans, J., and J. P. Fortuin (1992), Sensitivity of glaciers and small ice caps to greenhouse warming, *Science*, *258*(5079), 115–117, doi:10.1126/science.258.5079.115.
Palazzi, E., J. V. Hardenberg, and A. Provenzale (2013), Precipitation in the Hindu-Kush Karakoram Himalaya: Observations and future scenarios, *J. Geophys. Res. Atmos.*, *118*, 85–100, doi:10.1029/2012JD018697.
Pohl, E., M. Knoche, R. Gloaguen, C. Andermann, and P. Krause (2015a), Sensitivity analysis and implications for surface processes from a hydrological modelling approach in the Gunt catchment, high Pamir Mountains, *Earth Surf. Dyn.*, *3*(3), 333–362, doi:10.5194/esurf-3-333-2015.
Pohl, E., R. Gloaguen, and R. Seiler (2015b), Remote sensing-based assessment of the variability of winter and summer precipitation in the Pamirs and their effects on hydrology and hazards using harmonic time series analysis, *Remote Sens.*, *7*(8), 9727–9752, doi:10.3390/rs70809727.
Probst, J., and Y. Tardy (1987), Long range streamflow and world continental runoff fluctuations since the beginning of this century, *J. Hydrol.*, *94*(3-4), 289–311, doi:10.1016/0022-1694(87)90057-6.
Schaake, J. C., and C. Liu (1987), Development and application of simple water balance models to understand the relationship between climate and water resources, in *New Directions for Surface Water Modeling Proceedings of the Baltimore Symposium, May 1989, IAHS Publ., 181*, 343–352.
Schaefli, B., and M. Huss (2011), Integrating point glacier mass balance observations into hydrologic model identification, *Hydrol. Earth Syst. Sci.*, *15*(4), 1227–1241, doi:10.5194/hess-15-1227-2011.
Scherler, D., B. Bookhagen, and M. R. Strecker (2011a), Hillslope-glacier coupling: The interplay of topography and glacial dynamics in High Asia, *J. Geophys. Res.*, *116*, F02019, doi:10.1029/2010JF001751.
Scherler, D., B. Bookhagen, and M. R. Strecker (2011b), Spatially variable response of Himalayan glaciers to climate change affected by debris cover, *Nat. Geosci.*, *4*(3), 156–159, doi:10.1038/ngeo1068.
Schiemann, R., M. G. Glazirina, and C. Schär (2007), On the relationship between the Indian summer monsoon and river flow in the Aral Sea basin, *Geophysical Research Letters*, *34*, L05706, doi:10.1029/2006GL028926.
Skamarock, W. C., and J. B. Klemp (2008), A time-split nonhydrostatic atmospheric model for weather research and forecasting applications, *J. Comput. Phys.*, *227*(7), 3465–3485, doi:10.1016/j.jcp.2007.01.037.
Sorg, A., T. Bolch, M. Stoffel, O. Solomina, and M. Beniston (2012), Climate change impacts on glaciers and runoff in Tien Shan (Central Asia), *Nat. Clim. Change*, *2*(10), 725–731, doi:10.1038/nclimate1592.
Sproles, E. A., S. G. Leibowitz, J. T. Reager, P. J. Wigington, J. S. Famiglietti, and S. D. Patil (2015), GRACE storage-runoff hystereses reveal the dynamics of regional watersheds, *Hydrol. Earth Syst. Sci.*, *19*(7), 3253–3272, doi:10.5194/hess-19-3253-2015.
Stahl, K., R. D. Moore, J. M. Shea, D. Hutchinson, and A. J. Cannon (2008), Coupled modelling of glacier and streamflow response to future climate scenarios, *Water Resour. Res.*, *44*, W02422, doi:10.1029/2007WR005956.
Strahler, A., D. Muchoney, J. Borak, M. Friedl, S. Gopal, E. Lambin, and A. Moody (1999), MODIS Land Cover Product Algorithm Theoretical Basis Document (ATBD) Version 5.0, Cent. for Remote Sens., Dep. of Geogr., Boston University, Boston, Mass.
Swenson, S., and J. Wahr (2006), Post-processing removal of correlated errors in GRACE data, *Geophys. Res. Lett.*, *33*, L08402, doi:10.1029/2005GL025285.
Tahir, A. A., P. Chevallier, Y. Arnaud, and B. Ahmad (2011), Snow cover dynamics and hydrological regime of the Hunza River basin, Karakoram Range, Northern Pakistan, *Hydrol. Earth Syst. Sci. Discuss.*, *8*(2), 2821–2860, doi:10.5194/hessd-8-2821-2011.
Tangdamrongsub, N., S. C. Steele-Dunne, B. C. Gunter, P. G. Ditmar, and A. H. Weerts (2015), Data assimilation of GRACE terrestrial water storage estimates into a regional hydrological model of the Rhine River basin, *Hydrol. Earth Syst. Sci.*, *19*(4), 2079–2100, doi:10.5194/hess-19-2079-2015.
Tarasova, L., M. Knoche, J. Dietrich, and R. Merz (2016), Effects of input discretization, model complexity, and calibration strategy on model performance in a data-scarce glacierized catchment in central Asia, *Water Resour. Res.*, *52*, 4674–4699, doi:10.1002/2015WR018551.
Thenkabail, P. S., and Z. Wu (2012), An Automated Cropland Classification Algorithm (ACCA) for Tajikistan by Combining Landsat, MODIS, and secondary data, *Remote Sens.*, *4*(12), 2890–2918, doi:10.3390/rs4102890.
Unger-Shayesteh, K., S. Vorogushyn, D. Farinotti, A. Gafurov, D. Duethmann, A. Mandychev, and B. Merz (2013), What do we know about past changes in the water cycle of Central Asian headwaters? A review, *Global Planet. Change*, *110*, 4–25, doi:10.1016/j.gloplacha.2013.02.004.
United Nations, Department of Economic and Social Affairs, Population Division (2015), *Demographic Components of Future Population Growth: 2015 Revision*, New York. [Available at: http://www.un.org/en/development/desa/population/theme/trends/dem-comp-change.shtml, accessed 1 Dec. 2016.]
Varis, O. (2014), Resources: Curb vast water use in central Asia, *Nature*, *514*(7520), 27–9, doi:10.1038/514027a.
Wan, Z. (2008), New refinements and validation of the MODIS Land-Surface Temperature/Emissivity products, *Remote Sens. Environ.*, *112*(1), 59–74, doi:10.1016/j.rse.2006.06.026.
Wan, Z., and Z.-L. Li (1997), A physics-based algorithm for retrieving land-surface emissivity and temperature from EOS/MODIS data, *IEEE Trans. Geosci. Remote Sens.*, *35*(4), 980–996, doi:10.1109/36.602541.
Wan, Z., Y. Zhang, Q. Zhang, and Z. L. Li (2004), Quality assessment and validation of the MODIS global land surface temperature, *Int. J. Remote Sens.*, *25*(1), 261–274, doi:10.1080/0143116031000116417.
Werth, S., A. Güntner, S. Petrovic, and R. Schmidt (2009), Integration of GRACE mass variations into a global hydrological model, *Earth Planet. Sci. Lett.*, *277*(1–2), 166–173, doi:10.1016/j.epsl.2008.10.021.